Physics – Uspekhi **43** (4) 365 – 380 (2000)

REVIEWS OF TOPICAL PROBLEMS PACS numbers: **75.25.+z**, 75.30.Cr, **76.60.–d**

Influence of quantum fluctuations on the magnetic properties of quasi-one-dimensional triangular antiferromagnets

B S Dumesh

DOI: 10.1070/PU2000v043n04ABEH000636

Contents

Abstract. A review is presented of the experimental work on the influence of quantum fluctuations on the magnetization and the mean spin of magnetic sublattices in quasi-one-dimensional triangular antiferromagnets. The principal results in this area are the strong magnetic-field dependence of magnetic sublattice mean spins; anisotropy of mean spin values in magnetically nonequivalent antiferromagnetic chains; the reduction of magnetization compared to the classical spin case; the nonlinear growth of the parallel magnetic susceptibility; a residual magnetization anisotropy at high fields. The results obtained are explained based on the spin-wave theory of quantum fluctuations in antiferromagnets. A new magnetic phase was observed in $CsMnI_3$ for $H \,||\, C_6$ and shown to be due to the anisotropy of the mean spins of the sublattices.

1. Introduction

The problem of determining the ground magnetic state of antiferromagnetic insulators has a long and dramatic history. The simplest theory, developed by Louis Néel, describes this state by the antiparallel ordering of neighboring magnetic moments with definite values of the mean spin at each site of the magnetic lattice, $\langle S\rangle = S$ (the spin of the magnetic ion). However, one can easily show that the wave function corresponding to this state is not an eigenstate of the Heisenberg exchange interaction operator. Borovik-Romanov very clearly explains the essence of the problem [1]: "The state of ideal antiferromagnetic order of a crystal lattice does not correspond to the minimum of the lattice energy. The reason is that, in contrast to the ferromagnetic case, an interchange of two neighboring spins in an antiferromagnet (AF), disturbs the strict order in the alternating spins. Thus, the very nature of the exchange interaction makes the state with strong separation of the spins into two sublattices unstable."

The wave function of a true ground state can be represented as an expansion in the orthonormal set of wave functions corresponding to a definite set of spin flips. Here, the modulus of the mean value of the projection of the site spin on the quantization axis, $\langle S\rangle$, is smaller than the nominal spin value S. Such spin flips reduce the energy $\mathscr{E}$, although the diagonal part of the exchange energy increases [2]:

$$-NjS^2z > \mathscr{E}_g > -NjS^2z\left(1+\frac{1}{zS}\right). \qquad (1)$$

Here, the left-hand side is the energy of the Néel state, N is the total number of spins, and z is the number of nearest neighbors.

For many years this phenomenon, known as spin reduction in antiferromagnets, has attracted the attention of both theoreticians and experimenters. The procedure of calculating spin reduction can be illustrated with the example of a simple Hamiltonian with Heisenberg exchange interaction and single-ion anisotropy:

$$\mathscr{H} = 2\sum_{i,j} j_{ij}\hat{\vec{S}}_i\hat{\vec{S}}_j - D\sum_i (\hat{S}_z^2)^2 . \qquad (2)$$

B S Dumesh Institute of Spectroscopy, Russian Academy of Sciences
142092 Troitsk, Moscow region, Russian Federation
Tel. (7-095) 334-02 39
E-mail: dumesh@isan.troitsk.ru

Received 3 July 1999, revised 9 February 2000
Uspekhi Fizicheskikh Nauk **170** (4) 403 – 418 (2000)
Translated by E Yankovsky; edited by S N Gorin

To determine the ground state of this system, one must first use the Holstein – Primakoff transformation to expand the state in spin-wave creation and annihilation operators (a_k^+, a_k),

$$H' = \sum_k A_k a_k^+ a_k + \frac{1}{2}\sum_k (B_k a_k^+ a_{-k}^+ + B_k^* a_k a_{-k}) , \qquad (3)$$

and then find the ground state by diagonalizing this Hamiltonian (the Bogolyubov transformation). The result is the following expression for $\Delta S = S - \langle S\rangle$ [2]:

$$\Delta S = \frac{1}{2}\int \left(\frac{A_k}{\hbar\omega(k)} - 1\right) \mathrm{d}k , \qquad (4)$$

where

$$h\omega(k) = \left(A_k^2 - |B_k|^2\right)^{1/2} \qquad (5)$$

is the spin-wave energy. Thus, the reduction of mean spins in antiferromagnets is related to spin-wave quantum fluctuations.

The degree of the spin reduction for three-dimensional antiferromagnets is not large. According to Anderson's calculations [2] for a simple cubic lattice, $\Delta S \approx 0.078$, i.e., the effect is noticeable only for small spins, $S = 1/2$. However, it is difficult to interpret experiments with such ions (Cu^{2+}) due to the complexity of exactly allowing for orbital effects, which are of order $g - 2$ (here g is the electron gyromagnetic ratio) and are comparable to the sought spin reduction. The situation is much simpler for ions in the S state, such as Fe^{3+} and Mn^{2+} ($^6S_{5/2}$), but for these ions the reduction is only 3 to 5%.

There are two regular methods of measuring the mean values of magnetic moments: one uses the amplitude of the Bragg peaks of elastic neutron scattering, and the other uses the values of the hyperfine fields at the nuclei of the magnetic ions. The accuracy of the first method is limited by the need to allow for extinction effects (attenuation and rescattering) in the neutron beam and usually does not exceed 3 to 5%. The accuracy of measuring hyperfine fields and the magnetic resonance involving the nuclei of magnetic ions in magnetic insulators is roughly ten times higher. But to calculate $\langle S\rangle$, one needs to independently determine the hyperfine constant A. This constant is found from the hyperfine splitting of the EPR spectrum of the same ion incorporated as a weak impurity into a nonmagnetic matrix isomorphic to the given substance (e.g., $MnO \leftrightarrow Mg_{0.999}Mn_{0.001}O$). However, the accuracy of measuring the hyperfine constant is also too low for studying fine effects.

As a result of this complex experimental situation, the interest in the problem of spin reduction in antiferromagnets waned considerably in the 1970 – 1980s, and we know of no reviews on this topic published in the period between the mid-seventies and 1993 [3]. The problem of measuring spin reduction began its 'second life' at the end of the 1980s in connection with experiments involving quasi-one-dimensional antiferromagnets, where the related effects proved to be much larger and reliably observable in neutron scattering experiments. Moreover, calculations of integrals of type (4) are much simpler when $j'/j \leqslant 10^{-2}$ (here, j' is the interchain exchange). The results of calculations involving square and triangular lattices with allowance for kinematic interaction [4] and of comparison with the experimental data on five quasi-one-dimensional antiferromagnets were given by Welz [3] and were found to coincide within 10%.

In view of the large spin reduction in quasi-one-dimensional antiferromagnets, it became possible to investigate higher-order effects, specifically, the field dependence of the mean spin. The qualitative features of the effect of a magnetic field on $\langle S\rangle$ are readily revealed by equation (4). Here, the poles of the integrand, i.e., the region $\omega_e(k) \approx 0$, contribute substantially to the reduction. When a field is applied, gaps appear in the spin-wave spectrum and the magnitude of the integral (and spin reduction, respectively) diminishes. This effect, known as suppression of quantum fluctuations by a magnetic field, has been under intensive theoretical study in recent years. From the viewpoint of experimenters, this type of study is preferable, since it reduces to relative measurements, which have higher accuracy.

Spin reduction and, correspondingly, the effects associated with suppression of quantum fluctuations have a greater magnitude in quasi-one-dimensional triangular antiferromagnets. We will see that quantum fluctuations not only lead to sizable renormalization of the magnetic parameters of these substances but also initiate new magnetic phase transitions. The present review is devoted to these subjects. The plan is as follows. Section 2 discusses the magnetic properties of these compounds. Section 3 deals with the results of magnetization measurements in $CsMnBr_3$ and $CsNiCl_3$, where for the first time the effects of suppression of quantum fluctuations were found. Section 4 describes measurements of the mean spins of Mn^{2+} ions and the field dependence of these spins in $CsMnBr_3$, $RbMnBr_3$, and $CsMnI_3$ using the ^{55}Mn NMR, and the new magnetic phase discovered in the last substance. Section 5 interprets the results on mean-spin measurements and the mean-spin field dependence. The nature of the new magnetic phase is discussed in Section 6.

2. Magnetic properties of quasi-one-dimensional triangular antiferromagnets

2.1 Magnetic structures and phase diagrams

About two dozen compounds with the chemical formula ABX_3 belong to the class of quasi-one-dimensional antiferromagnets with a triangular magnetic structure (here, A is Rb or Cs, B is an atom of a transition metal, and X is a halogen atom). All these antiferromagnets have a similar crystallographic structure [5] (Fig. 1). The B^{2+} ions are surrounded by octahedrons of halogen atoms, which, being connected via a common face, form chains along the C_6 axis. These chains are hexagonally packed in the basal plane of the crystal, while the voids that are formed in the process are filled by atoms of the alkali metal. The unit cell consists of two formula units; its symmetry is D_{6h}^4. Crystallographically, all the B^{2+} ions are equivalent.

The distance between neighboring B^{2+} ions along the chain is approximately half the distance between neighboring ions in the plane. Accordingly, the exchange integral j involving neighboring ions in the chain is several hundred times larger than the interchain exchange integral j'. Here, we will examine only the case where both exchanges are antiferromagnetic. Due to the interchain exchange (j'), magnetic ordering emerges in these substances at $T \approx 10$ K. Here, the spins of the B^{2+} ions in the chains are ordered antiferromagnetically, while the mutual polarization of the

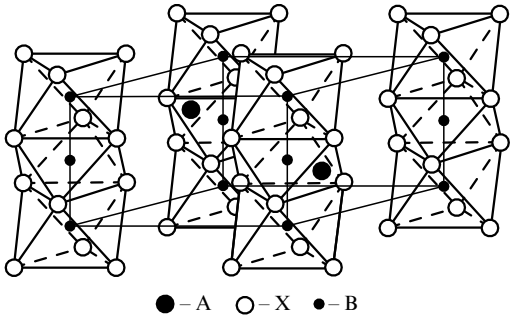

Figure 1. Crystal structure of ABX_3-type quasi-one-dimensional triangular antiferromagnets.

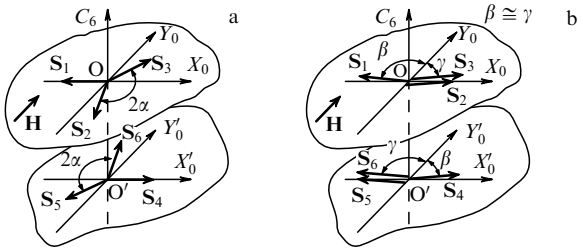

Figure 2. Low-temperature magnetic structure of quasi-one-dimensional triangular antiferromagnets with strong easy-plane anisotropy ($CsMnBr_3$) for $|H| \ll H_C$ (a) and $|H| > H_C$ (b).

chains is determined by j' and the crystal anisotropy. Due to a frustration of the AF exchange on a flat hexagonal grid, six-sublattice triangular magnetic structures are realized in these substances: in weak fields, the spins of the neighboring B^{2+} ions in the plane lie on the sides of isosceles triangles.

Due to the nontrivial nature of such magnetic structures, much attention has been paid to their studies. For instance, in their review of magnetic properties of such substances, Collins and Petrenko [6] mention about 300 studies. To the first approximation, the magnetic properties of these compounds with V, Mn, and Ni ions are described by the model Heisenberg Hamiltonian of a system of equivalent spins with allowance for single-ion anisotropy and the Zeeman energy of the magnetic moments in an external magnetic field H:

$$\mathscr{H} = 2j\sum_i S_i S_{i+\Delta_x} + 2j'\sum_i S_i S_{i+\Delta_\perp} + D\sum_i (S_i^z)^2 - g\mu_B H\sum_i S_i\,, \tag{6}$$

where g is the Landé g factor, μ_B is the Bohr magneton, $j > 0$ and $j' > 0$ are the integrals representing the antiferromagnetic exchange interaction, and D is the anisotropy constant. The first term on the right-hand side describes the exchange interaction along the C_6 axis, and the second term describes the exchange interaction in the plane perpendicular to C_6.

In $CsMnBr_3$ and in the vanadates, $D > 0$ (easy-plane anisotropy), with the result that the spins of B^{2+} are oriented in the hexagonal plane of the sample and in a zero magnetic field form regular triangles. Since the anisotropy in this plane is negligible, in weak magnetic fields the spin structure orients itself in such a way that one of the bisectors of the triangle is directed along $H_\perp$ (Fig. 2) (the field projections are designated in relation to the C_6 axis).

The behavior of easy-plane triangular antiferromagnets in a strong magnetic field is determined by the ratio of the interchain exchange j' to the anisotropy. The compound $CsMnBr_3$ (and $RbMnBr_3$, which will be discussed later) is a case of strong anisotropy: $D > 3j'$. Hence, for any magnetic fields applied in the basal plane, all the spins of Mn^{2+} lie in this plane, and the spin triangle is deformed in such a way that the angle at its base decreases according to the law [7]

$$\cos\alpha = \frac{1}{2-z}\,, \quad z = \frac{H^2}{H_C^2}\,, \tag{7}$$

vanishing in a field $H_C = (48jj')^{1/2}S$ (for $CsMnBr_3$, $H_C = 64$ kOe at $T = 1.8$ K [8]). In such a field (H_C), a second-order phase transition occurs to a collinear structure consisting of antiferromagnetically ordered ferrimagnetic planes with a spin ratio of 2:1. When the magnetic field does not lie in the hexagonal plane, the position of the transition is given by the formula

$$H_C^2(\phi) = H_C^2\frac{d-1}{d\cos^2\phi - 1}\,, \tag{8}$$

where $d = D/3j'$, and ϕ is the angle between the field and the hexagonal plane. The magnetic structure and phase diagram of $CsMnBr_3$ have been thoroughly studied via magnetization and neutron scattering measurements [8–11][1].

In nickelates and $CsMnI_3$, $D < 0$ (easy-axis anisotropy), with the result that the spins of B^{2+} tend to align themselves along the C_6 axis. However, the interchain exchange (j') obstructs the formation of such a collinear structure. A real magnetic structure is the result of a trade-off between anisotropy and exchange. Here, in a third of the AF chains, the spins are directed along the C_6 axis (spins S_A), while the remaining spins (S_B) make an angle with the axis given by the equation [6]

$$\cos\Theta = \frac{1}{2 - D/3j'}\,. \tag{9}$$

In this way, a coplanar six-sublattice magnetic structure[2] is created in which the antiferromagnetic chains (A and B) are magnetically nonequivalent (Fig. 3). In a zero magnetic field, the spin plane can freely rotate with respect to the C_6 axis, while in a nonzero field it rotates in such a way that its normal becomes parallel to $H_\perp$.

When $H \,||\, C_6$, such a structure is energetically unfavorable, and in a field $H_{sf} \approx (16DjS^2)^{1/2}$ a spin-flop transition occurs, as a result of which all spins of B^{2+} are oriented in the hexagonal plane. When the external field makes an angle with the C_6 axis, the rotation of the spin plane proceeds gradually, so that [13]

$$\tan 2\psi = \frac{H^2\sin 2\varphi}{H^2\cos 2\varphi - H_{sf}^2}\,, \tag{10}$$

where ψ is the angle between the normal $\mathbf{n}$ to the spin plane and the C_6 axis, and φ is the angle between H and C_6 (Fig. 3b).

A direct transition from the paramagnetic phase to the low-field phase is impossible; so, the two phases are separated

[1] The critical properties of triangular antiferromagnets were discussed in Kawamura's review [12].

[2] We will call the plane to which the spins of B^{2+} are parallel the spin plane.

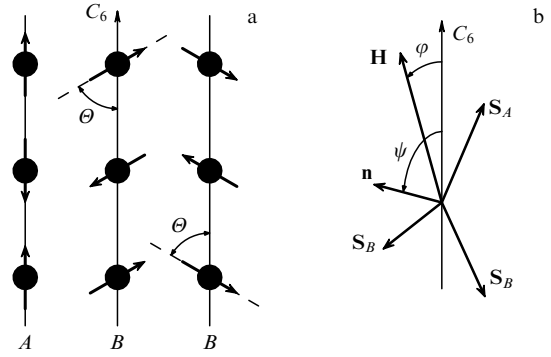

Figure 3. Low-field magnetic structure of easy-axis quasi-one-dimensional triangular antiferromagnets (a), and the position of the spin plane in relation to the magnetic field and the crystallographic axes (b).

by an intermediate phase, in which only the spin projections on the C_6 axis are ordered. Accordingly, there are two Néel temperatures, T_{N1} and T_{N2}. All three magnetically ordered phases and the paramagnetic phase coexist in a single multicritical point ($T_m = 10$ K and $H_m = 60$ kOe for $CsMnI_3$). Thus, we have described the $H-T$ phase diagram of easy-axis triangular antiferromagnets, which for $CsMnI_3$ is depicted in Fig. 4 [14].

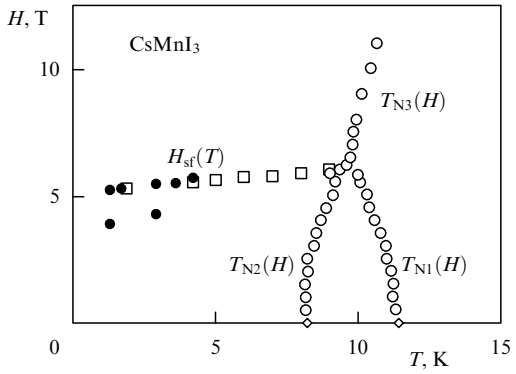

Figure 4. Magnetic phase diagram of $CsMnI_3$ for $H||C_6$: ○ and □ represent the data of Katori et al. [14], and • represent the data extracted from the ^{55}Mn NMR spectrum.

The magnetic susceptibility of triangular antiferromagnets in weak fields is anisotropic. This anisotropy is conveniently described by the phenomenological parameter $\eta = (\chi_{||} - \chi_\perp)/\chi_\perp$, where $\chi_{||}$ and $\chi_\perp$ are the susceptibilities in fields parallel and perpendicular to the normal to the spin plane, respectively. For classical spins,

$$\chi_\perp = \frac{1}{16Dj}\,, \quad \eta = 1\,. \tag{11}$$

Below, we discuss the specific features of susceptibility associated with suppression of quantum fluctuations by a magnetic field.

2.2 Antiferromagnetic resonance

The resonance properties of triangular AFs have been studied fairly thoroughly. Here, we will discuss only the results of studies of low-lying modes of antiferromagnetic resonance (AFMR) in easy-plane compounds with strong anisotropy ($CsMnBr_3$) and easy-axis substances. Chubukov [7] and Tanaka et al. [15] developed the theory of AFMR in easy-plane triangular antiferromagnets, while Zaliznyak et al. [16] and Kimura et al. [17] conducted experiments with $CsMnBr_3$. There exists a gapless (Goldstone) AFMR mode ω_{e1} (in the notation of Ref. [16]) related to torsional vibrations of the spin triangle. For $H\,||\,C_6$, we have $\omega_{e1} = 0$, while for $H \perp C_6$, the frequency of this mode in weak fields is given by the expression

$$\frac{\omega_{e1}}{\gamma_e} = \frac{\sqrt{3}}{2}\,\frac{H^3}{H_C^2}\,. \tag{12}$$

As $H \to H_C$, we have $\omega_{e1} \to \gamma_e H_C$, and after the transition we obtain $\omega_{e1} = \gamma_e H$. When the field strength is intermediate, there is no analytical expression for ω_{e1}, and the spectrum is calculated using an equation derived by Chubukov [7].

Furthermore, there is a respiratory AFMR mode ω_{e5} related to vibrations of the angle at the vertex of the spin triangle. At $H = 0$ the frequency $\omega_{e5} \approx 190$ GHz ($CsMnBr_3$). However, as $H \to H_C$, the gap in this branch tends to zero according to the law

$$\omega_{e5}^2 = \gamma_e^2 (H_C^2 - H^2)\,. \tag{13}$$

Only spins that are directed obliquely to the magnetic fields participate in this mode and the mode is excited only when the dc and hf magnetic fields are parallel [15]. Both modes have been observed in experiments, and the spectra are in satisfactory agreement with the theoretical results. The other AFMR branches in $CsMnBr_3$ are fairly high.

In easy-axis triangular antiferromagnets, there are three AFMR modes whose activation nature is related to the relativistic anisotropy or the external magnetic field [13, 18]. In the present review, we mainly follow the work of Abarzhi et al. [13], who base the theory of antiferromagnetic resonance on the macroscopic dynamics of magnetic substances [19].

One of the modes (e_2 in the notation of Abarzhi et al. [13]) corresponds to the torsional vibrations of the spin plane in relation to the C_6 axis and is gapless in a zero field. Its spectrum is given by the equation

$$\omega_{e2}^2 = \gamma_e^2\,\frac{\eta}{2}\left[(H^4 + H_{sf}^4 - 2H^2 H_{sf}^2 \cos 2\varphi)^{1/2} + H^2 - H_{sf}^2\right], \tag{14}$$

which becomes much simpler when $H \ll H_C$:

$$\frac{\omega_{e2}}{\gamma_e} = \frac{\sqrt{\eta}\,H H_{sf} \sin\varphi}{\sqrt{H_{sf}^2 - H^2}}\,. \tag{15}$$

What is important is that only the spins S_B participate in this mode.

The gaps in the other modes are determined by relativistic invariants of the second order

$$\omega_{e1}^2(0) = \gamma_e^2 \eta H_{sf}^2 \tag{16}$$

and sixth order (the mode e_3). Since there are four such invariants, the behavior of ω_{e3} in a field is fairly arbitrary:

$$\omega_{e3}^2(H) = \frac{\gamma_e^2}{\chi_\perp}\,\frac{36\eta}{1+\eta}\,\frac{H_{sf}^2 - H^2}{\eta H_{sf}^2 + H^2}\,F(H)\,, \tag{17}$$

where

$$F(H) = b_1 + b_2H^2 + b_3H^4 + b_4H^6 . \qquad (18)$$

The relativistic invariants of the sixth order also determine the orientation of the spin triangles in the spin plane and can be calculated for systems described by the Hamiltonian (6). The calculations of Abarzhi et al. [13] at $H \,||\, C_6$ yield

$$F(H) = \frac{D^3S^2}{216j'^2}\left(1 - \frac{H^2}{H_{sf}^2}\right)^3 . \qquad (19)$$

The AFMR spectra measured in the experiments of Zaliznyak et al. [16] for $CsNiCl_3$ and of Abarzhi et al. [13] and Kambe et al. [20, 21] for $CsMnI_3$ are in fairly good agreement with the results of calculations, but for the second substance the value of D/j' obtained from the gap ratio ω_{e1}/ω_{e3} differs substantially from that derived from the spin-triangle angle [equation (9)].

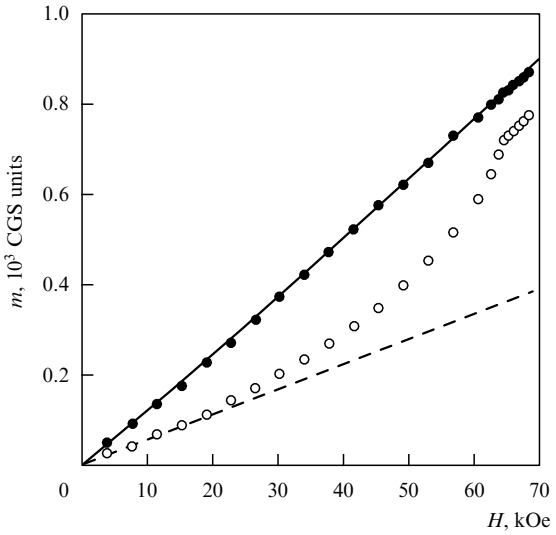

Figure 6. Field dependence of the magnetization of $CsMnBr_3$ for $H \perp C_6$ (○) and $H \,||\, C_6$ (●) [8]. The solid curve represents the results of calculations and the dashed line is the low-field asymptote [25].

3. Quantum fluctuations and magnetization

3.1 Influence of quantum fluctuations on the magnetization

Quantum fluctuations and their suppression by a magnetic field greatly affect the magnetic properties of quasi-one-dimensional magnetic materials. This effect manifests itself most strikingly in the renormalization of the constants in the spin Hamiltonian (6) and in the substantial difference between the magnetization values and those calculated for classical spins [equation (11)]. Figures 5 and 6 show the field dependence of the magnetizations of $CsMnBr_3$ and $CsNiCl_3$ measured at low temperatures by Abarzhi et al. [8] and Zaliznyak [22]. Note three special features of this dependence: the small value of magnetizations compared to the limit for classical spins; the nonlinear growth of $m_\perp$ in a strong magnetic field, which is especially noticeable for $CsNiCl_3$; and the residual anisotropy of magnetization above the reorientational phase transition. Zaliznyak [22] related the first feature to the renormalization of the constants in the spin Hamiltonian and the second, to the field-induced increase of the mean spins of the magnetic sublattice caused by suppression of spin fluctuations. The data on the magnetization were used by Zaliznyak [22] to calculate the field behavior of the mean spins. In the next section, we will see that the order of the effect was determined correctly but that reality proved to be much more interesting.

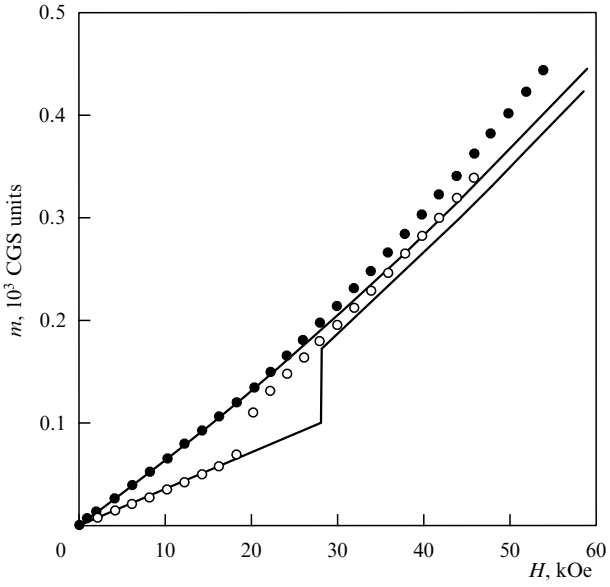

Figure 5. Field dependence of the magnetization of $CsNiCl_3$ for $H \,||\, C_6$ (○) and $H \perp C_6$ (●) [22]. The solid curves represent the results of calculations done by Zhitomirsky and Zaliznyak [25].

The magnetization anisotropy was also explained by Abanov and Petrenko [23] by allowing for quantum corrections to the ground state of quasi-one-dimensional triangular antiferromagnets. More thorough numerical calculations were done by Ohyama and Shiba [24], while analytical calculations were done by Zhitomirsky and Zaliznyak [25]. According to the analytical calculations, in easy-plane quasi-one-dimensional triangular antiferromagnets, the quantum corrections to $\langle S\rangle$ and m for the case where $H \,||\, C_6$ are given by the equations

$$\langle S\rangle = S\left\{1 - \frac{1}{2\pi S}\left[\ln\frac{16j}{3j'} - \pi - \frac{1}{2}\langle\ln(1-\gamma_k)\rangle - \frac{1}{2}\left\langle \ln\left(1 + 2\gamma_k + \frac{D}{3j'} + \frac{H^2}{48jj'S^2}\right)\right\rangle\right]\right\},$$

$$m = \frac{H}{8j}\left\{1 - \frac{1}{2\pi S}\left[\ln\frac{16j}{3j'} - 2 - \frac{1}{2}\left\langle \ln\left(1 + 2\gamma_k + \frac{D}{3j'} + \frac{H^2}{48jj'S^2}\right)\right\rangle\right]\right\}, \qquad (20)$$

where $\gamma_k = (1/3)(\cos k_x + 2\cos k_x/2 \cos k_y)$, and the averaging is done over the two-dimensional Brillouin zone. The numerical values in the isotropic case, $\langle\ln(1-\gamma_k)\rangle = -0.176$ and $\langle\ln(1+2\gamma_k)\rangle = -0.452$, are fairly small, and for $j \gg j'$ the main additional term $\ln(16j/3j')$ is common to both equations. What is essential is that the term with the field dependence is normalized to the reorientational transition field H_C, which is fairly moderate in triangular antiferromagnets. Hence, the field effects become appreciable in fields $H \approx H_C$. Zhitomirsky and Zaliznyak [25] also calculated the

field dependence of $m_{||}$ and $m_{\perp}$ for easy-axis triangular antiferromagnets (the solid curves in Fig. 5). We see that the results of the experiment involving $CsMnBr_3$ are described quite well by the theory, while those involving $CsNiCl_3$ are described only qualitatively. The discrepancy may be due to the relatively high temperature (compared to $T_N = 4.4$ K) at which the experiment with this substance took place ($T = 1.8$ K). The numerical calculations of the field behavior of the mean spins and the magnetization in $CsNiCl_3$ done by Ohyama and Shiba [24] correlate sufficiently well with the results of Zhitomirsky and Zaliznyak [25].

Thus, the theory of suppression of quantum fluctuations by a magnetic field provides a good description of the field dependence of magnetization in triangular antiferromagnets. However, since magnetization is an integral characteristic and, generally, depends on many parameters, there could be other explanations of the observed phenomena. Hence, the direct measurements of spin reduction and its field dependence are quite important.

3.2 Anisotropy of spin reduction in nonequivalent antiferromagnet chains

There is an interesting effect that has been predicted for easy-axis triangular antiferromagnets but cannot be observed in direct magnetization measurements. Watabe et al. [26] used a numerical construction of Bogolyubov's transformations to calculate spin reduction in easy-axis triangular antiferromagnets and found that this reduction is different for magnetically nonequivalent AF chains of the same substance. Figure 7 depicts the results of spin reduction calculations for a model hexagonal structure with the Hamiltonian

$$\mathscr{H} = 2j' \sum_i S_i S_{i+\Delta_\perp} + D \sum_i (S_i^z)^2 \qquad (21)$$

depending on the anisotropy-to-exchange constant ratio $D/2j'$. In the easy-axis case ($D > 0$) with $D/2j' < 1.3$, the reduction for spins S_A parallel to the symmetry axis is smaller than for the other spins. The change of sign of the reduction difference at high anisotropy is due to the approach of the transition to the collinear structure at $D/2j' = 1.5$.

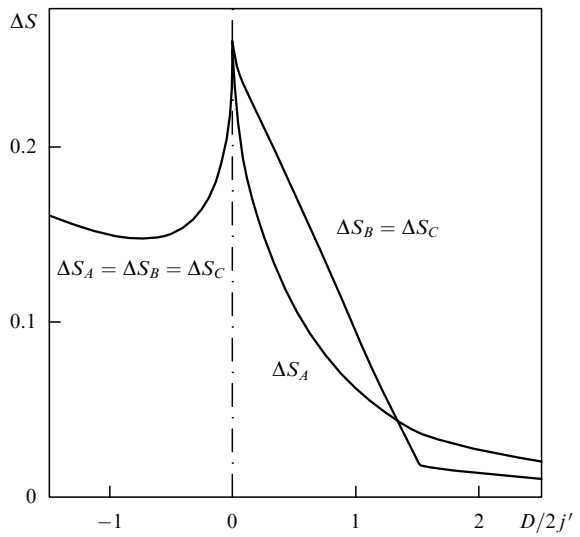

Figure 7. Reduction of mean spins for a model triangular system depending on the anisotropy-to-exchange constant ratio [26].

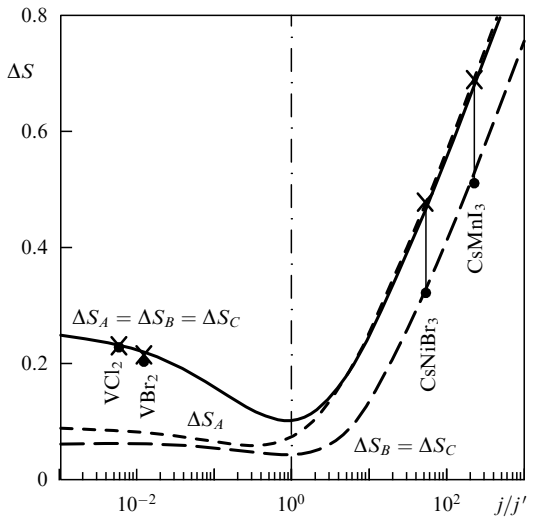

Figure 8. Dependence of mean-spin reduction in six-sublattice triangular antiferromagnets on the exchange-constant ratio. The solid curve corresponds to $D/2j' = 0$ and the dashed curves to $D/2j' = 1$ [26].

Figure 8 illustrates the calculation of spin reduction for a real six-sublattice antiferromagnetic structure (the Hamiltonian (6) with a zero magnetic field) depending on the exchange-constant ratio j/j' at $D/2j' = 0$ (solid curve) and $D/2j' = 1$ (dashed curves). Clearly, for quasi-one-dimensional antiferromagnets ($j/j' > 0$) (including $CsMnI_3$), the difference in spin reduction in nonequivalent AF chains is substantial. This effect can easily be understood by using the linear theory of spin reduction in antiferromagnets. For the spins S_B, there is a pole in the integral (4) that is related to the vanishing of the electron spin mode e_2. Since the spins S_A do not participate in this mode, the magnitude of the integral and, respectively, the reduction is smaller for these spins.

In what follows, we will show that the real anisotropy in this substance is much smaller. Nevertheless, the predicted effect is interesting enough to merit attempts at detecting it in experiments. Moreover, there is a need to study the process of suppression of spin reduction by a magnetic field directly. To this end, ^{55}Mn NMR in $CsMnBr_3$, $RbMnBr_3$, and $CsMnI_3$ was investigated. We will devote the remainder of the review to this aspect.

4. ^{55}Mn NMR in quasi-one-dimensional triangular antiferromagnets

4.1 Features of NMR in multisublattice antiferromagnets

The main contribution to the effective field at the nuclei of magnetic ions is provided by the hyperfine interaction. The hyperfine field caused by this interaction for 3d ions is $\mathbf{H}_{ni} = A\langle \mathbf{S}_i \rangle \approx 10^2 - 10^3$ kOe, where A is the hyperfine constant, and $\langle \mathbf{S}_i \rangle$ is the mean spin of the ith magnetic sublattice. The NMR frequencies are determined by the effective field, which is the vector sum of the hyperfine and external magnetic fields at a given nuclei:

$$\frac{\omega_{ni}}{\gamma_n} = |\mathbf{H}_{ni} + \mathbf{H}| \,. \qquad (22)$$

We see that the NMR frequencies in a zero field determine the mean spins of the sublattices, while the field splitting determines the angle between the spins and the field. The

complex magnetic structure of triangular antiferromagnets leads to a rich NMR spectrum. For instance, for $H \perp C_6$, the ^{55}Mn NMR spectrum in the triangular phase of $CsMnBr_3$ consists of three twofold degenerate branches,

$$\frac{\omega_{ni}}{\gamma_n} = |\mathbf{H}_{ni} + \mathbf{H}| \approx \begin{cases} H_n \pm H\sin\alpha\,, \\ H_n\,, \end{cases} \tag{23}$$

while in the collinear phase all the branches merge:

$$\omega_n \approx \gamma_n H_n \left(1 + \frac{H^2}{H_n^2} - 2\,\frac{H_\perp^2}{H_n H_E}\right)^{1/2} \approx \gamma_n H_n\,. \tag{24}$$

For the sake of simplicity, equation (23) is reduced to an approximation that is linear in H. The quadratic terms have also been taken into account in calculations of the spectrum.

For the low-frequency phase of $CsMnI_3$, the NMR spectrum generally consists of two nondegenerate (for the spins S_A) and two twofold degenerate (for the spins S_B) branches:

$$\begin{cases} \dfrac{\omega_{Ai}}{\gamma_n} = H_{nA} \pm H_{||}\,, \\ \dfrac{\omega_{Bi}}{\gamma_n} = H_{nB} \pm H_{||}\cos\Theta\,. \end{cases} \tag{25}$$

Here, $H_{||} = H\sin(\psi - \varphi)$ is the projection of the field on the spin plane.

The real NMR spectrum is much more complex at low temperatures due to the interaction with the low-lying AFMR branches. This phenomenon emerges because of the effect of nuclear spins on the motion of the electron moment due to the same hyperfine interaction and has become known as the dynamic shift of the NMR frequency (pulling). The theory of the phenomenon for two-sublattice antiferromagnets was built by de Gennes et al. [27], who showed that the frequency shift is proportional to the mean nuclear magnetization $\langle m_n\rangle = \chi_n H_n$:

$$\Omega_n = \omega_n\left[1 - 2\left(\frac{\omega_T}{2\omega_e}\right)^2\right], \tag{26}$$

where Ω_n is the realistic NMR frequency, $\omega_T = \gamma_e(2H_E A\langle m_n\rangle)^{1/2}$ is the coupling frequency, and H_E is the exchange field. The equation is valid for $\omega_T/\omega_e \ll 1$. Since the coupling incorporates a strong exchange field, for some manganese-based antiferromagnets the dynamic NMR frequency pulling already manifests itself at $T = 4.2$ K. Later, Turov and Kuleev [28] derived an equation for the spectrum of coupled vibrations of the electron and nuclear moments in two-sublattice antiferromagnets over the entire frequency range:

$$(\omega_{ej}^2 - \Omega^2)(\omega_n^2 - \Omega^2) - (\omega_T\Omega)^2 = 0\,. \tag{27}$$

This equation provides a good description of all the known examples of the NMR frequency pulling due to the interaction of a single NMR mode with different AFMR modes ω_{ej} in two-sublattice antiferromagnets [29].

The dynamic frequency pulling for several NMR modes has been calculated for only two special cases: a classical antiferromagnet with two nonequivalent positions of nuclear spins [30], and an easy-plane triangular antiferromagnet in weak fields [31, 32]. In Ref. [33], an equation combining these two cases of dynamic NMR frequency pulling was proposed:

$$\omega_{ej}^2 - \Omega^2 = \frac{\Omega^2\omega_T^2}{\Sigma\rho_i}\sum_{i=1}^{m}\frac{\rho_i}{\omega_{ni}^2 - \Omega^2}\,, \tag{28}$$

where ρ_i is the number of spins (per unit magnetic cell) in the ith NMR mode, and m is the number of these modes. This equation provides a good description of all the known experimental examples of the dynamic frequency pulling of several NMR modes [30, 33–37] and at $i = 1$ becomes the Turov equation (27). It has one electron-like solution $\Omega_{ej}^2 = \omega_{ej}^2 + \omega_T^2$ and m nucleus-like solutions satisfying the condition $\omega_{n\,i-1} < \Omega_{ni} < \omega_{ni}$. Only the lower branch of the NMR spectrum, Ω_{nm}, is shifted considerably; for $\omega_{nm}\omega_T^2/\omega_{ej}^2 \gg \omega_{n1} - \omega_{nm}$ this branch is described by an equation close to the nuclear-like solution (27):

$$\Omega_{nm}^2 = \tilde{\omega}_{n0}^2\,\frac{1}{1 + \omega_T^2/\omega_{ej}^2}\,, \tag{29}$$

where

$$\tilde{\omega}_{n0}^{-2} = \frac{1}{\Sigma\rho_i}\sum_{i=1}^{m}\rho_i\,\omega_{ni}^{-2}\,. \tag{30}$$

Thus, to describe coupled electron–nuclear vibrations in multisublattice antiferromagnets, one needs only a single additional constant ω_T, which can easily be found from the value of the temperature-dependent gap in the AFMR spectrum. For $CsMnBr_3$, it was found by Zaliznyak et al. [31], and for $CsMnI_3$, by Prozorova et al. [38]. Below, we will show that a good description of the experimental NMR spectra is provided by the theory of dynamic frequency pulling with these constants.

The NMR technique in strong fields, which are discussed in the sections that follow, also has its own special features. To excite a spin-echo signal in an ordinary pulse spectrometer, the following condition must be met:

$$\gamma_n\eta_{rf}h\tau \approx \frac{\pi}{2}\,,$$

where h is the amplitude of the hf field, τ is the pulse length, and $\eta_{rf} \approx H_n/H$ is the gain. For ordinary $\tau \approx 1$ μs and $\eta_{rf} < 10$, it is difficult to attain the required field amplitudes $h \approx 10^2$ kOe. At the same time, the optimum condition for observing continuous NMR,

$$\gamma_n\eta_{rf}h\sqrt{T_1T_2} \approx 1\,,$$

where T_1 and T_2 are the longitudinal and transverse relaxation times, respectively, is satisfied at realistic field strengths of 1–10 Oe. Therefore, the experiments discussed below were done with a continuous NMR spectrometer [39].

4.2 ^{55}Mn NMR in $CsMnBr_3$

Experiments with $CsMnBr_3$, $RbMnBr_3$, and $CsMnI_3$ were done with single crystal samples grown by S V Petrov at the Kapitza Institute of Physics Problems of the Russian Academy of Sciences using the Bridgman method. The samples were oriented along natural cleavage planes (binary planes). To impede hydration, the samples were covered by a protecting film of rubber cement and kept in a helium atmosphere.

NMR measurements were made with a continuous modulation spectrometer of the type described in Ref. [39] with removable cavities in the frequency range 200–500 MHz

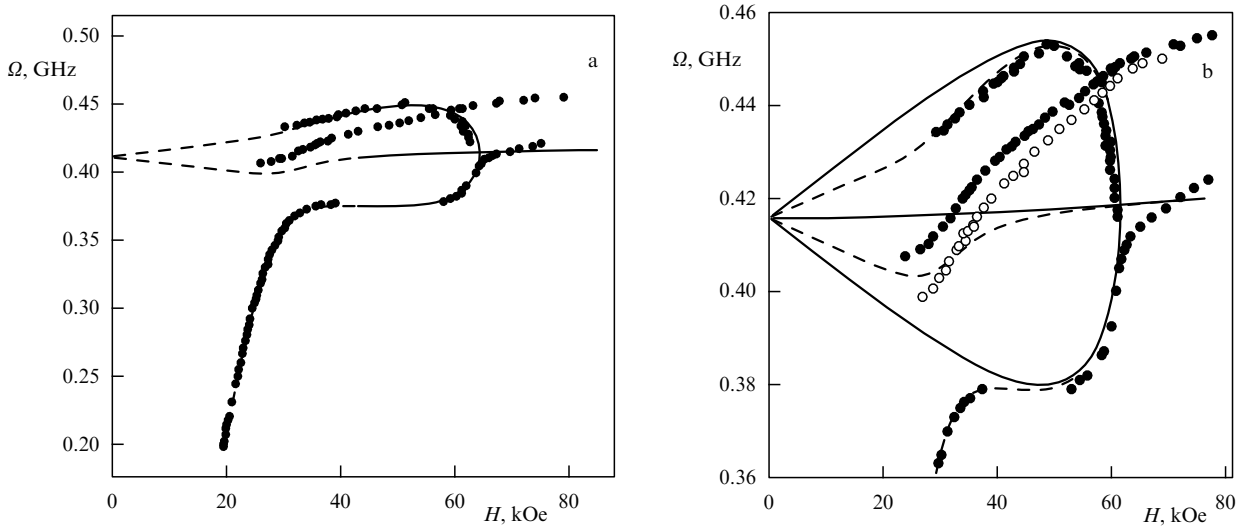

Figure 9. (a) ^{55}Mn NMR spectrum of $CsMnBr_3$ for $H \perp C_6$ at $T = 1.3$ K (•). (b) The same on a larger scale and the spectrum of the middle branch at $T = 3.0$ K (○). The solid lines represent the unshifted spectrum and the dashed lines represent the same spectrum with allowance for the dynamic shift of the NMR frequency [35].

and the temperature range 1.3–4.2 K (basically, at $T = 1.3$ K). A magnetic field up to 80 kOe was generated by a small superconducting solenoid (with an inner diameter of 20 mm) and measured by a Hall probe. The probe was calibrated by the NMR signal from hydrogen in a film of the rubber cement protecting the sample. The nonuniformity of the field on the sample, determined by the width of the ^{1}H NMR, was smaller than 10^{-3}. Due to the fairly strong dependence of the ^{55}Mn NMR frequencies on the magnetic field, most of the measurements were made by turning the magnetic field through resonance .

The ^{55}Mn NMR signal in $CsMnBr_3$ was observed for $H \perp h \perp C_6$. Usually it consisted of several lines of different widths ($\Delta\omega \approx 0.5-4$ MHz) and intensities. The ^{55}Mn NMR spectrum at $T = 1.3$ K is displayed in Fig. 9 [35]. For $H < 63$ kOe, three NMR branches are observed. These branches correspond to the triangular magnetic structure of $CsMnBr_3$. In fields lower than 45 kOe all, these branches are distorted due to the interaction with the Goldstone AFMR mode [see equation (12)]. The solid lines in Fig. 9 correspond to the unshifted NMR frequencies [calculations using equations (23) and (24)] with $\omega_{n0} = 416$ MHz, and the dashed curves correspond to the spectrum with allowance for dynamic frequency pulling at $\omega_T = 6$ GHz. Clearly, the calculations provide a good description of the behavior of the upper and lower branches of the spectrum up to the reorientational transition. The position of the middle branch in weak fields is close to the calculated one, but as the field increases, the branch frequency increases anomalously. After the transition to the collinear phase, the rate of this increase is depressed. Above the transition, the position of the lower branch is, on the average, close to the calculated one, but an anomalous increase in the branch frequency is also evident.

The anomalies in the spectrum occur mainly in the range of fields where the dynamic NMR frequency pulling for ^{55}Mn is negligible. The only possible explanation for these anomalies is the increase in $H_n(H)$, which is different for magnetically nonequivalent AF chains. The field dependence of the hyperfine fields at the ^{55}Mn nuclei in $CsMnBr_3$ is depicted in Fig. 10 [40]. In the next section, we will show that the hyperfine field is unambiguously related to $\langle S \rangle$. Thus,

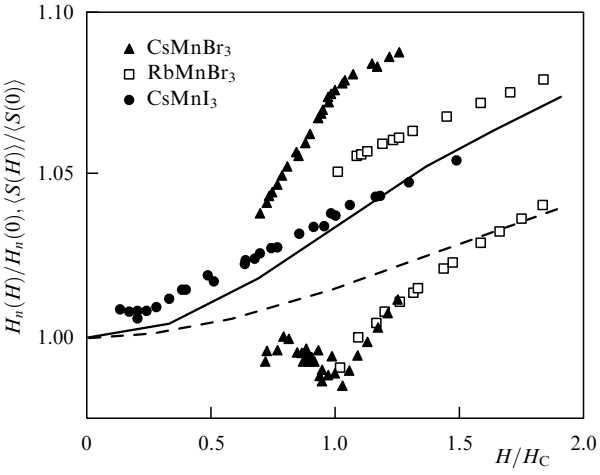

Figure 10. Field dependence of the mean spins of AF chains in $CsMnBr_3$, $RbMnBr_3$, and $CsMnI_3$ (the spins S_B) for $H \perp C_6$. The field is normalized to the field of the transition to the collinear or spin-flop phase [40]. The solid curve corresponds to the results of calculations by Ohyama and Shiba [24], and the dashed curve corresponds to those by Zhitomirsky and Zaliznyak [25].

suppression of spin reduction by a magnetic field is indeed observed, but it is different for nonequivalent AF chains. The value of the average spin of magnetic sublattices, $\langle S \rangle = 1.80 \pm 0.05$, determined from the value $\omega_{n0} = 416 \pm 4$ MHz and the hyperfine constant of Mn^{2+} [41] obtained from the data on EPR in isomorphic $CsMgBr_3$, correlates well with the neutron diffraction data of Gaulin et al. [10] and the results of Zhitomirsky and Zaliznyak's calculations [25]. The main contribution to the error is provided by the inaccuracy in measuring the hyperfine constant A.

Since for $H > 40$ kOe the corrections introduced by the dynamic NMR frequency pulling are small, from the field dependence of the upper and lower NMR branches one can directly determine the angles between the magnetic sublattices and the magnetic field. The fact that the measured and calculated spectra coincide corroborates the validity of

Chubukov's predictions [7] concerning the field dependence (7) of the angles of the triangle. Note that this experiment yielded the first direct observation of field deformations of triangular structures in this class of antiferromagnets.

4.3 ^{55}Mn NMR in $CsMnI_3$

The ^{55}Mn NMR spectrum of $CsMnI_3$ takes on the simplest form when $H \perp C_6$ ($\varphi = 90°$). In this geometry, all the spins of Mn^{2+} are perpendicular to the magnetic field, and the unshifted NMR spectrum consists of two (with allowance for $\langle S_A \rangle \neq \langle S_B \rangle$) degenerate branches. The strong frequency pulling can be observed only in weak fields, since the frequency of the Goldstone AFMR mode rapidly increases with field strength, $\omega_{e2} = \gamma_e \sqrt{\eta} H$, and the ω_{e3} mode in this geometry lies fairly high ($\omega_{e3} = \text{const} = 34$ GHz) and interacts only weakly with NMR.

When $H \perp C_6$, only one ^{55}Mn NMR branch with strong dynamic frequency pulling was observed. The spectrum of this branch at $T = 1.3$ K is depicted in Fig. 11 [40]. It can be assumed that, in this geometry, the gain of the hf field for the other NMR branches is too small. Since in this case only one nuclear mode interacts with only one electron mode, the NMR spectrum is described by the Turov equation (27), with the coupling frequency ω_T being determined in AFMR measurements [38]. The only free parameter $\omega_{nB}(0) = 388$ MHz can easily be determined from the slope of the curve representing the field dependence of the NMR frequency in weak fields.

The spectrum calculated by equation (27) is represented as the dashed curve in Fig. 11. Clearly, the results of calculations provide a good description of the experimental data for magnetic fields up to 7 kOe, i.e., in the region where the dynamic NMR frequency pulling plays an important role. In stronger fields, the NMR frequency experiences a considerable increase. This growth is much larger than the quadratic corrections to the unshifted NMR frequency (the solid curve in Fig. 11) and is related to the field dependence of the hyperfine field $H_{nB}(H)$, i.e., to the suppression of spin reduction by the magnetic field.

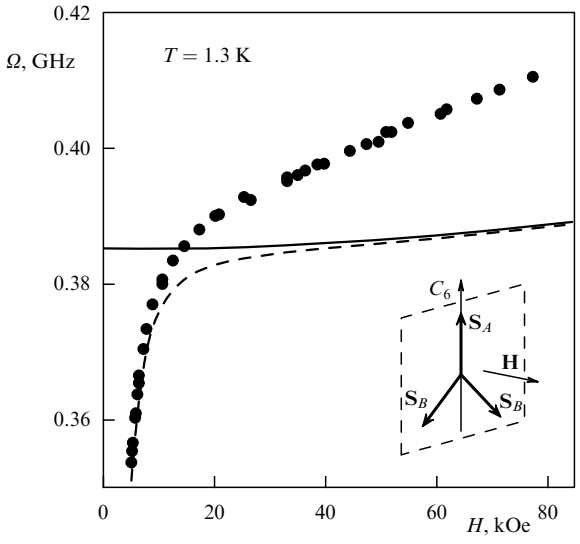

Figure 11. Lower branch of the ^{55}Mn NMR spectrum of $CsMnI_3$ for $H \perp C_6$ at $T = 1.3$ K (•). The solid line represents the unshifted spectrum, and the dashed line represents the same spectrum with allowance for the dynamic NMR frequency pulling [40].

^{55}Mn NMR in $CsMnI_3$ for $H \perp C_6$ in magnetic fields up to 10 kOe was observed independently by Kubo et al. [42], who used the spin-echo method. They detected two ^{55}Mn NMR branches, which grew with the field. The spectrum of one of these branches ($\Omega_{n1} \approx 200 - 380$ MHz) was found to be in good agreement with the data of Borovik-Romanov et al. [40]. We did not, however, detect the second NMR branch with frequencies $\sim 2\Omega_{n1}(H)$. This branch appears to be rather strange; e.g., it corresponds to an anomalously large mean spin of Mn^{2+} $\langle S \rangle = 3.1$. We believe that Kubo et al. [42] observed only one NMR branch excited both at the natural frequency and at double frequencies. For instance, in $MnCO_3$, which also exhibits a dynamic NMR frequency pulling, spin-echo at ^{55}Mn was observed in the event of excitation by two pulses with a frequency $2\Omega_n$. The echo signal was also registered at $2\Omega_n$ [43].

Much richer is the ^{55}Mn NMR spectrum of $CsMnI_3$ measured at small angles between the external field and the C_6 axis. At such angles, all six possible NMR modes corresponding to the six spins of Mn^{2+} in the unit cell are observed. The spectrum of five of these modes is shown in Fig. 12 for $H \parallel C_6$ [36] (in this geometry, the frequency of the sixth mode is zero, but it is observed when H deviates from the C_6 axis). The spectrum is fairly complex, but the main features of the magnetic structure of $CsMnI_3$ are clearly visible. For instance, as $H \to 0$, the modes with the strong field dependence converge to $\omega_{n1} = 417$ MHz and those with the weak field dependence to $\omega_{n2} = 388$ MHz. Thus, nonequivalent AF chains really have different $\langle S \rangle$. For $H < 39$ kOe, the experimental data are in good agreement with the calculated spectra for the low-field phase (the solid curves in Fig. 12). The NMR frequencies are used to determine the mean spins of AF chains: $\langle S_A(0) \rangle = 1.86 \pm 0.1$ and $\langle S_B(0) \rangle = 1.74 \pm 0.1$. Here, we only give the error caused by the inaccuracy of determining the NMR frequency. The uncertainty in the value of the hyperfine constant amounts to 4% [41]. The NMR results correlate well with the neutron diffraction data $\langle S(0) \rangle = 1.8$ [45, 46].

Above 52.5 kOe, only one NMR mode is observed. This means that all the spins of Mn^{2+} are equal and are positioned equivalently with respect to the external magnetic field, i.e., the well-known high-field phase is realized in such fields. The

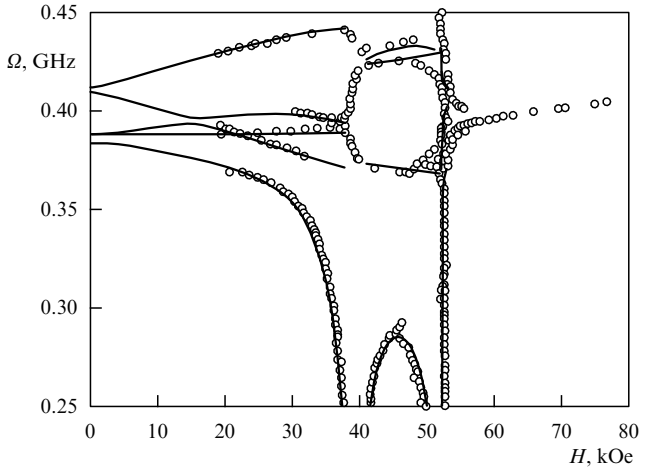

Figure 12. ^{55}Mn NMR spectrum of $CsMnI_3$ for $H \parallel C_6$ at $T = 1.3$ K (○). The solid lines represent the calculations with allowance for the dynamic shift of the NMR frequency [44].

position of the transition coincides with that given by the data extracted from static measurements (see Fig. 4). The transformation of NMR spectra reflects the characteristic features of a spin-flop transition: a sudden transformation into a single branch, the presence at H_{sf} of absorption with a width of roughly 0.2 kOe within a broad frequency range (the nearly vertical branch in Fig. 12), and the existence of a singularity only for small angles $\varphi < 1^\circ$. This means that the rotation of the spin plane to a position perpendicular to the external field is sudden.

At $H_C = 39$ kOe, all NMR branches undergo a drastic transformation, which means that there is a phase transition into a new magnetic phase. The transition is retained even when the field makes an angle with the C_6 axis of up to 15°. Some of the features of the spectrum (the divergence of three upper NMR modes above H_C, and rapid softening near H_C of the NMR mode related to ω_{e3}) indicate that, at H_C, a reorientation of the spins within the spin plane occurs. Only two symmetric orientations of the spin triangles are possible here: one of the sides is parallel to the C_6 axis (the low-field phase of $CsMnI_3$), or one of the bisectors is parallel to this axis (similarly to $CsMnBr_3$). Both phases are schematically depicted in Fig. 13. A detailed calculation of the NMR spectra (the solid curves in Fig. 12) based on the magnetic structure of phase *3* shows that the phase is indeed realized for 39 kOe $< H <$ 52.5 kOe. This is corroborated by studies of ^{55}Mn NMR spectra when the field deviates from the C_6 axis [36]. The measured transition fields H_C are shown in the phase diagram of $CsMnI_3$ (Fig. 4).

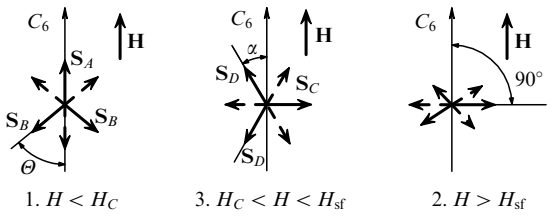

Figure 13. Low-temperature magnetic phases (*1–3*) of $CsMnI_3$ for $H \parallel C_6$.

Prior to the ^{55}Mn NMR studies, no phase *3* was observed, since the magnetization of $CsMnI_3$ at H_C has no singularities and the AFMR mode ω_{e3} in this phase has very low frequencies and thus are inconvenient for observation. Neither is there any neutron scattering data in this range of fields.

Although the results of calculations of the dynamic NMR frequency pulling provide a fairly good description of the experimental spectra, their accuracy is insufficient for exposing the fine details of the magnetic structure. To this end it is more convenient to measure the unshifted NMR modes directly. In $CsMnI_3$, these modes are realized when the field deviates from the C_6 axis. Here, the frequency of the AFMR mode ω_{e2} rapidly increases [equations (14) and (15)], and for the related NMR modes the dynamic frequency pulling becomes unimportant in relatively weak magnetic fields. Under these conditions, from the NMR spectra one can directly determine (without additional constants) the values of the hyperfine fields and the angles between the magnetic sublattices. For instance, in phase *3* the unshifted NMR spectrum consists of three twofold degenerate branches whose frequencies in the linear approximation in H/H_n are expressed by the equations (the notation C and D correspond to Fig. 13)

$$\frac{\omega_D^{+-}}{\gamma_n} = H_{nD} \pm H\cos\alpha\sin(\psi-\varphi)\,, \quad \frac{\omega_C}{\gamma_n} = H_{nC}\,, \tag{31}$$

where 2α is the angle between the directions of the spins of neighboring AF chains D, and ψ is the angle between the normal to the spin plane and the external field.

In phase *3* at $\varphi \approx 7^\circ$, we have $\omega_{e2}^2 \gg \omega_T^2$, and for the NMR branches interacting with this mode the dynamic frequency shift is negligible. From the spectra of these branches, we can determine the hyperfine fields $H_{nC} = \omega_C/\gamma_n$ and $H_{nD} = (\omega_D^+ + \omega_D^-)/2\gamma_n$ and the angles between the spins S_D and the field:

$$\cos\alpha\sin(\psi-\varphi) = \frac{\omega_D^+ - \omega_D^-}{2\gamma_n H}\,. \tag{32}$$

In phase 3 the difference between the angles of the spin triangle and 60° is small; as a result, $\psi(H)$ can be calculated using (32). This dependence is displayed in Fig. 14 [47]. The values of $\langle S(H)\rangle$ calculated from those of the hyperfine fields are shown in Fig. 15 [47].

The NMR spectra at large angles between the field and the C_6 axis are used in a similar way to determine the hyperfine

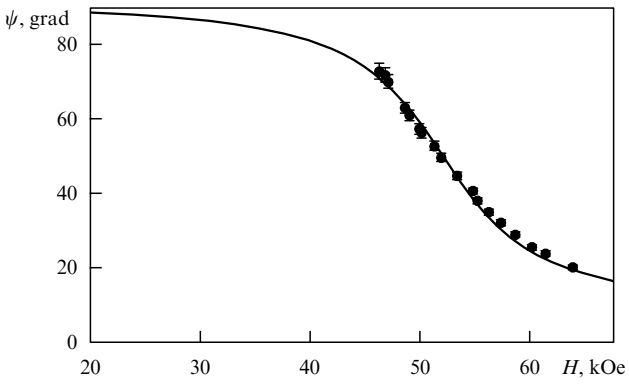

Figure 14. Field dependence of the angle between the normal to the spin plane and the C_6 axis in $CsMnI_3$ at $\varphi = 7^\circ$ [47]. The solid curve represents the results of calculations using equation (10).

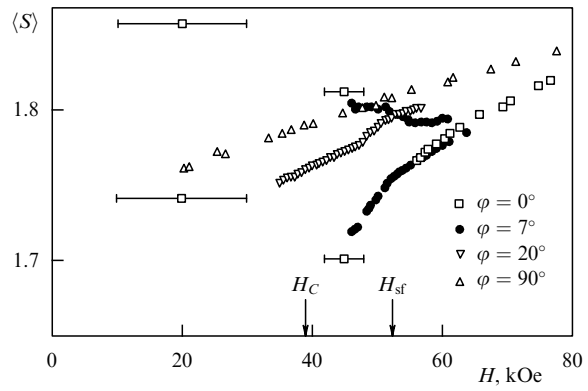

Figure 15. Field dependence of the mean spins in $CsMnI_3$ for different orientations of the magnetic field [47] (▽ and △ correspond to $\langle S_B\rangle$)).

fields and the angles between the spins in the low-field phase *1*. For instance, Fig. 16 shows the field-induced deformation of the spin triangle in the low-field phase obtained from the NMR spectra at $\varphi \approx 20^\circ$. The field dependence of the mean spins of the magnetic sublattices found in these experiments is analyzed in the next section.

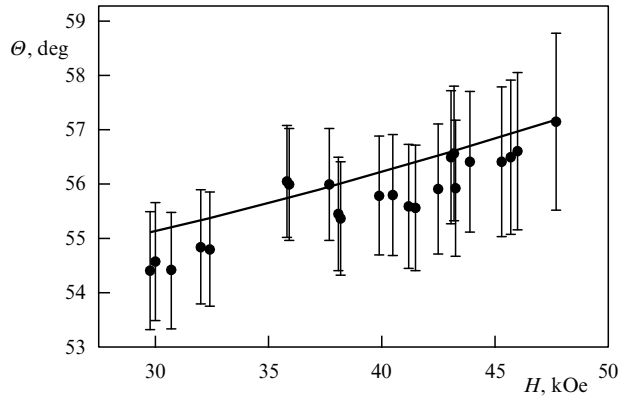

Figure 16. Field dependence of the angle at the base of the spin triangle in the low-field phase of $CsMnI_3$ (at $\varphi = 20^\circ$) [47]. The solid curve represents the results of calculations done using Eqn (38).

4.4 ^{55}Mn NMR in $RbMnBr_3$

^{55}Mn NMR in $RbMnBr_3$ was studied within the same cycle of investigations. In its structural and magnetic properties, this substance is a distorted analog of $CsMnBr_3$. At room temperature, the structure of $RbMnBr_3$ is described by the same symmetry group D^4_{6h}. However, at roughly 150 K, orthorhombic distortions arise [48] that greatly affect the magnetic properties of this substance.

The magnetic properties of $RbMnBr_3$ have been studied in much detail by the elastic [49] and inelastic [49, 50] neutron scattering methods, by measuring the static magnetization [51], and by the antiferromagnetic resonance method [52]. Below $T_N = 8.5$ K, the spins in the chains become ordered antiferromagnetically and align themselves along the basal plane in the same way as in $CsMnBr_3$. However, the mutual orientation of the chains is much more complicated. In weak magnetic fields, a magnetic structure that is incommensurate with the crystal lattice appears in this substance, with the angle of rotation of the neighboring spins in the basal plane depending on the magnetic field.

At $H \approx 30$ kOe (we consider the case where $H \perp \widetilde{C}_6$)[3], a first-order phase transition to a commensurate triangular magnetic structure occurs (a characteristic feature of this transition is hysteresis). As the field is further increased, a second-order phase transition to a collinear structure similar to the high-field phase of $CsMnBr_3$ occurs at $H_{C2} = 41$ kOe.

Experiments on ^{55}Mn NMR in $RbMnBr_3$ were carried out by the same method as in $CsMnBr_3$ and $CsMnI_3$. In all the experiments, the dc and hf magnetic fields were in the basal plane of the sample and were mutually perpendicular.

The ^{55}Mn NMR signal was observed only in the commensurate phases of $RbMnBr_3$ in a frequency range of 350–450 MHz and in magnetic fields of 30–80 kOe at $T = 1.3$–4.2 K. It can be assumed that in the incommensurate phase of $RbMnBr_3$ there is no amplification of the NMR signal and there is not enough sensitivity to detect the signal. The ^{55}Mn NMR spectrum for $H \perp \widetilde{C}_6$ is shown in Fig. 17 [32] and is easily reproducible from sample to sample. No anisotropy in the basal plane is observed. Neither is there a dynamic NMR frequency pulling; this is quite natural, since the effect of the Goldstone AFMR mode in fields $H > 30$ kOe is small. The solid curves in Fig. 17 represent the unshifted NMR spectrum calculated using equations (23) and (24).

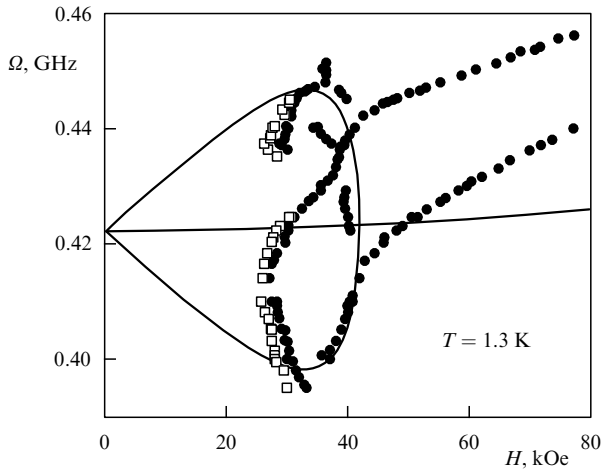

Figure 17. ^{55}Mn NMR spectrum of $CsMnI_3$ for $H \perp C_6$ at $T = 1.3$ K (•). The squares represent the position of the lines for the reverse course of the field in the hysteresis region, and the solid curves represent the unshifted spectrum [32].

Both phase transitions clearly manifest themselves in the NMR spectrum: the first, in the form of absorption (accompanied by hysteresis) over a broad range of frequencies near 30 kOe (in the hysteresis region, the centers of the absorption lines for the direct and reverse courses of the field are denoted by circles and squares, respectively), and the second, similarly to that in $CsMnBr_3$, via the merging of the upper and lower NMR branches. Generally, above H_{C1} the spectrum is qualitatively similar to that of $CsMnBr_3$. Indeed, in the triangular phase, three NMR branches are observed, with the middle branch being very strongly dependent on the magnetic field. As a result, only two branches remain in the collinear phase, with the frequency of the lower branch increasing with the field much more rapidly than that of the upper branch. In $RbMnBr_3$, this effect is much more evident, since the range of magnetic fields in which measurements can be carried out is much broader (with respect to H_{C2}). The field behavior of the hyperfine fields at ^{55}Mn nuclei in the collinear phase of $RbMnBr_3$ is depicted in Fig. 10. The NMR frequency in a zero field is $\omega_n(0) = 422 \pm 8$ MHz. The resulting mean spin with allowance for the hyperfine constant of $RbMnBr_3$ determined by Kirklin and McPherson [53], $\langle S(0) \rangle = 1.8 \pm 0.1$, coincides with the neutron diffraction data presented by Glinka et al. [49].

Thus, $\langle S(0) \rangle \approx 1.8$ in all the substances that were studied, which demonstrates the strong reduction of the spins of Mn^{2+} and correlates well with neutron diffraction data. All the substances exhibit a substantial increase in the hyperfine fields (mean spins) in a magnetic field and a difference in the values of these spins in magnetically nonequivalent AF

[3] In our notation of the axes, we adhere to the symmetry of the high-temperature phase.

chains. Moreover, a new magnetic phase has been discovered in $CsMnI_3$. We will show below that this phase exists because of the difference in the mean spins. In the next section, we will analyze the field dependence of the hyperfine fields (mean spins).

5. Spin reduction in Mn^{2+} and its suppression by a magnetic field in quasi-one-dimensional triangular antiferromagnets

Before we discuss the results of measurements of mean spins, let us study in greater detail the nature of the hyperfine constant of the Mn^{2+} ion and estimate the related uncertainties. Here, we will follow Ref. [54].

The main contribution to the hyperfine interaction in 3d ions is provided by core polarization, $H_p = A_p\langle S\rangle$, with the constant A_p negative [55]. The constant depends on the chemical environment of the ion, but for the same number and type of ligands the effect of the local symmetry and of the distance to the ligands is small. For instance, Ogawa [56] studied EPR at Mn^{2+} in many nonmagnetic fluorine compounds (coordination number six) and found that a change in the atomic separation by 10% induces a change in the hyperfine constant by only 2%.

The contribution of the orbital interaction to the hyperfine field was calculated by Abragam and Pryce [57]:

$$H_{nL} = 2\mu_B\left\langle\frac{1}{r^3}\right\rangle\Delta g_L = +125\left\langle\frac{1}{r^3}\right\rangle_{a.u.}\Delta g_L\,. \qquad (33)$$

Here H_{nL} is measured in kOe, $\langle 1/r^3\rangle$ is the mean reciprocal cube of the ion radius, and $\Delta g_L = g - 2$ is the orbital contribution to the g factor. The advantage of using Mn^{2+} ions is that Δg is small in such ions ($\Delta g \approx 0.004$ for $CsMnBr_3$ and $RbMnBr_3$, and $\Delta g \approx 0.008$ for $CsMnI_3$ [41, 53]). Hence, for these substances the orbital part of the hyperfine interaction (i.e., the part that depends on orientation) amounts to less than 1%.

The contribution to the hyperfine field from the surrounding magnetic ions [58, 59] is due to a transfer of the polarized spin density, i.e., it is of the same nature as the exchange interaction. For quasi-one-dimensional antiferromagnets, it is natural to divide it into two parts: the contribution from the neighbors within a chain, $H_{n\,tr}$, and the contribution from the neighbors in the plane, $H'_{n,tr}$. Here, $H'_{n,tr} \approx H_{n,tr}\,j'/j$, i.e., is insignificant. The part $H_{n,tr}$ is proportional to the number of nearest neighbors and, consequently, is three times smaller than the estimate made by Taylor and Owen [58] and Huang et al. [59]; it amounts to $H_{n,tr} \leqslant 1.5\%$. This part and the inaccuracy of EPR measurements of the hyperfine constant constitute the main source of the absolute error in determining the mean spins of the Mn^{2+} ions.

Now, we turn to the results of NMR experiments. First, we note that in $CsMnBr_3$ and $RbMnBr_3$ an increase in H_n is observed only for sublattices that are perpendicular to the magnetic field of the sublattices. Here, their position does not change in relation to the crystallographic axes and, hence, is independent of changes in A_L. The same is true of the field dependence of H_{nB} in $CsMnI_3$ for $H \perp C_6$. In general, the contribution to $H_n(H)$ can initiate a change in A_p related to magnetostriction. However, the magnetostriction in triangular antiferromagnets, measured in $CsNiCl_3$ by Raine et al. [60], is small ($\Delta l/l \approx 10^{-5}$), so that the field dependence of A_n is negligible. Hence, the relative error in determining $\langle S(H)\rangle$ for $CsMnBr_3$ and $RbMnBr_3$ amounts to approximately three parts in a thousand (the accuracy of determining the centers of the NMR lines).

The situation with $CsMnI_3$ is somewhat more complicated, since in this substance the directions of the magnetic sublattices in relation to the crystallographic axes change and the anisotropy of A_L is, generally, not small. Moreover, in some cases the information is extracted from NMR spectra deformed by the interaction, which affects the accuracy of determining H_n. For this substance, the relative error in determining $\langle S_i\rangle$ is approximately one part in a hundred, which is also much smaller than the observed effects.

Thermal fluctuations of the spins also contribute to $\langle S\rangle$. However, at $T \approx 1.3$ K they are small. For instance, from the data on the temperature dependence of H_n in $CsMnBr_3$ it follows that $\langle S(0)\rangle - \langle S(1.3\text{ K})\rangle \leqslant 0.01\langle S(0)\rangle$ [35]. Moreover, temperature fluctuations freeze out if $\hbar\omega_e(H) > kT$, i.e., in moderate magnetic fields. Figure 9b shows the field dependence of the frequencies of the middle ^{55}Mn NMR branch in $CsMnBr_3$ at $T \approx 1.3$ and 3 K. Clearly, the temperature addition, which is important in low fields, becomes insignificant when $H > 60$ kOe. Table 1 lists the values of $\langle S(0)\rangle$ obtained from ^{55}Mn NMR, from neutron diffraction data, and from theoretical calculations. Clearly, the results for $RbMnBr_3$ and $CsMnI_3$ are in good agreement with the neutron diffraction data (bearing in mind that the latter do not distinguish between $\langle S_A\rangle$ and $\langle S_B\rangle$ in $CsMnI_3$). For $CsMnBr_3$, the difference is significant, but one must take into account that the neutron diffraction measurements were made at a high temperature, $T \geqslant 4.2$ K. The spin reduction of Mn^{2+} in $CsMnBr_3$ measured by NMR is in good agreement with the results of Zhitomirsky and Zaliznyak's calculations [25].

Table 1.

Antiferromagnet	$\langle S(0)\rangle$		
	Neutron diffraction	NMR	Theory
$CsMnBr_3$	1.65 [9]	1.8 [40]	1.82 [25]
$RbMnBr_3$	1.8 [49]	1.8 [40]	
$CsMnI_3$	1.85 [45]	1.74; 1.86 [33]	2; 1.8 [26]

A new effect, predicted by Watabe et al. [26], has been detected in $CsMnI_3$: the difference in reduction for magnetically nonequivalent spins of Mn^{2+}. The order of the difference is $\langle S_A\rangle - \langle S_B\rangle \approx 0.12$, which is close to the calculated value (0.2) but of the opposite sign. We believe that this difference is due to the highly overvalued ratio of anisotropy to interchain exchange, $D/j' \approx 2$, used by Watabe et al. [26], while the experimental data on $CsMnI_3$ yield $D/j' \approx 0.6$ (see below). As noted in Section 3.2, the difference $\langle S_A\rangle - \langle S_B\rangle$ is extremely sensitive to this ratio and changes sign near the critical value $D/j' = 3$ (i.e., critical for the transition to the collinear phase). Thus, the experiment has demonstrated the difference (predicted in Ref. [26]) in spin reduction in magnetically nonequivalent AF chains of Mn^{2+} in $CsMnI_3$. A quantitative comparison would require a calculation with a realistic value of D/j' [4].

[4] When the present article was being reviewed, I received a letter [61] that contained the results of spin reduction calculations for $D/j' \approx 1$: $\langle S_A\rangle = 1.95$ and $\langle S_B\rangle = 1.80$, which is in good agreement with the present data.

In their work (initiated by the NMR results), Marchenko and Tikhonov [62] used the theory of exchange symmetry of magnetic materials [19] and obtained the relationships linking the values of the mean spins of Mn^{2+} for $CsMnI_3$ in phases *1* and *3*:

$$\text{phase } 1: \quad S_A = S(1+\Delta), \quad S_B = S\left(1-\frac{\Delta}{2}\right),$$
$$\text{phase } 3: \quad S_D = S\left(1+\frac{\Delta}{2}\right), \quad S_C = S(1-\Delta), \qquad (34)$$

where $(3/2)\Delta$ is the relative difference of spins at $H=0$. The experiment yields $S_A = 1.86 \pm 0.01$, $S_B = 1.74 \pm 0.01$, $S_D = 1.81 \pm 0.02$, and $S_C = 1.70 \pm 0.03$ [5]. (Here, we give only the error introduced by the inaccuracy of determining H_n.) Clearly, these results are in satisfactory agreement with (24).

Figure 10 shows (in relative units) the field dependence $\langle S(H)\rangle$ for all the triangular antiferromagnets studied by ^{55}Mn NMR with $H \perp C_6$. To make comparison easier, the magnetic field is normalized to the field of the reorientational phase transition (for $CsMnBr_3$ and $RbMnBr_3$, H_C is the field of transition to the collinear phase, and for $CsMnI_3$, H_{sf} is the spin-flop transition field).

Clearly, for the easy-plane antiferromagnets $CsMnBr_3$ and $RbMnBr_3$, the field behavior of $\langle S\rangle$ is similar: the splittings are of the same order and the slopes of the $\langle S(H)\rangle$ curves in the collinear phase are close in value, with the slope of the lower branches much larger than that of the upper branches. The observed minimum H_n in the vicinity of H_C for the lower branches is probably related to the inaccuracy of the model description of the NMR spectrum near the phase transition. The value of the splitting in the collinear phase is of the order of the difference $\langle S_A\rangle - \langle S_B\rangle$ for $CsMnI_3$. The increase in $\langle S_B\rangle$ for $CsMnI_3$ is close to linear, and the slope is close to that of the upper branches in the collinear phase of $CsMnBr_3$ and $RbMnBr_3$.

Quantitative comparison of the experimental results with the theory of suppression of quantum fluctuations by a magnetic field is hindered by the absence of calculations for the experimental situation. As far as we know, paper [26] by Watabe et al. is the only one where the possibility of different spin reductions is considered for crystallographically equivalent positions of the magnetic ions. Zhitomirsky and Zaliznyak [25] calculated $\langle S(H)\rangle$ for $CsMnBr_3$ [equation (20)], but only for $H \parallel C_6$ (the dashed curve in Fig. 10). In this geometry, all spins of Mn^{2+} are equivalent and there is no splitting. Below, we will show that this calculation corresponds to a lower bound on the observed effects. Nevertheless, it yields a correct order of magnitude for $\delta\langle S(H)\rangle$. In the class of easy-axis triangular antiferromagnets, the calculation for $H \perp C_6$ was done by Ohyama and Shiba [24] for $CsNiCl_3$. They assumed that at $H=0$ the reduction of all spins is the same. Their results are shown in normalized form $\langle S(H/H_{sf})\rangle/\langle S(0)\rangle$ by a solid curve in Fig. 10. Allowing for the fact that the results of the calculations depend on three constants (j, j', D), while H_{sf} depends only on two constants (j, D), we can state that the calculation and experimental results for $\langle S_B(H)\rangle$ in $CsMnI_3$ are in good agreement.

[5] An unfortunate mistake was made in Ref. [36] in the calculation of the mean spins for phase *3*: the hyperfine fields (given in that paper) were unnecessarily divided once again by γ_n, with the result that the values of $\langle S_C\rangle$ and $\langle S_D\rangle$ proved to be smaller than the correct values by a factor of 1.06.

The qualitative picture of the observed splitting can be obtained from the linear spin-reduction theory. Indeed, a significant contribution to integral (4) is provided by the regions near the bottom of the spin-wave band, i.e., spin waves with small k's and frequencies close to AFMR. In easy-plane antiferromagnets with $H \perp C_6$, there are two poles: one at $H=0$, where the Goldstone AFMR mode gap vanishes, and the other at $H = H_C$, where the frequency of the respiratory AFMR branch vanishes. When a magnetic field is applied, the frequency of the Goldstone branch increases in proportion to H^3, which leads to a substantial increase in $\langle S\rangle$. However, at the same time, for AF chains of Mn^{2+} that are directed obliquely to the field the value of $\langle S\rangle$ decreases, in view of which the frequency of the respiratory mode drops[6].

One can assume that these contributions are of the same order. Hence, in the triangular phase of easy-plane antiferromagnets there is a rapid increase of $\langle S(H)\rangle$ for AF chains perpendicular to the field, while the $\langle S(H)\rangle$ for obliquely directed chains is nearly constant. Above H_C, the increase in $\langle S(H)\rangle$ for the first type of chain is depressed, since $\omega_{e1} \propto H$ in the collinear phase, while for the second type of chain, $\langle S(H)\rangle$ increases rapidly, since the frequency of the respiratory mode grows rapidly. As noted earlier, the slope of $\langle S_B(H)\rangle$ for $CsMnI_3$ and that of $\langle S(H)\rangle$ in the collinear phase of $CsMnBr_3$ and $RbMnBr_3$ are close in value. This is quite natural, since in high fields for all three substances the gap in the spin-wave spectrum is $\omega(k=0) \approx \gamma_e H$.

For $H \parallel C_6$ in $CsMnBr_3$, we have $\omega_{e1}(H) \equiv 0$, with the result that the increase in $\langle S(H)\rangle$ is related only to the field dependence of the upper AFMR branches, whose contribution to integral (4) is substantially smaller. Hence, Zhitomirsky and Zaliznyak's result [25] can be considered the lower bound of our $\langle S(H)\rangle$ dependence.

The mean spins of the Mn^{2+} ions in different positions in $CsMnI_3$ and their field dependence for different angles between the field and the C_6 axis are shown in Fig. 15. At $\varphi \approx 0°$, the field dependence of $\langle S\rangle$ in phases *1* and *3* is weak and does not exceed experimental accuracy. Here, only the field dependence of $\langle S\rangle$ in the spin-flop phase is appreciable. At $\varphi \approx 7°$, $\langle S_D(H)\rangle$ is only weakly field-dependent, while $\langle S_C(H)\rangle$ is strongly dependent. This situation resembles the case of easy-plane triangular antiferromagnets with a strong field dependence of the spins that are perpendicular to the field. In strong fields the $\langle S\rangle$ for small φ practically coincide. Moreover, Fig. 15 depicts the $\langle S_B(H)\rangle$ calculated from unshifted NMR spectra at $\varphi \approx 20°$ and $\varphi \approx 90°$. Note that all the $\langle S(H)\rangle$ converge in high fields.

These results can be explained qualitatively on the basis of the field behavior of the low-lying AFMR modes ω_{e2} and ω_{e3} in $CsMnI_3$ and their effect on integral (4). For $\varphi \approx 0$ and $H < H_{sf}$, we have $\omega_{e2} \equiv 0$, while ω_{e3} in low fields is weakly dependent on H. Hence, in phase *1* both $\langle S_A\rangle$ and $\langle S_B\rangle$ remain practically unchanged up to the vicinity of H_C. The field behavior of $\langle S_B\rangle$ at $\varphi \approx 20°$ and $\varphi \approx 90°$ (phase *1*) is related to the increase in ω_{e2}.

The slower increase of $\langle S_B\rangle$ in weak fields at $\varphi = 20°$ in comparison to that at $\varphi = 90°$ is due to the weaker field dependence of ω_{e2} [equations (14) and (15)]. However, as we approach H_{sf}, the increase of ω_{e2} at $\varphi \approx 20°$ becomes more rapid, and for $H \gg H_{sf}$ its anisotropy tends to zero. Accord-

[6] An experiment that showed that the only sublattices that participate in the respiratory mode are those directed obliquely to the field is discussed in Ref. [37].

ingly, in high fields the anisotropy of the mean spins of Mn^{2+} decreases.

Thus, the main features of the field dependence of the mean spins in $CsMnI_3$ can be explained qualitatively. We may hope that microscopic calculations will yield quantitative agreement with the experimental data.

6. The nature of the intermediate magnetic phase in $CsMnI_3$

What is left to explain is the appearance of the new phase *3* in $CsMnI_3$. Note that theoreticians [63–65] have constructed various models of the intermediate phase in easy-axis triangular antiferromagnets. However, such phases are related to the reorientation of the spin plane in relation to the crystallographic axes, while the new phase differs from the low-field phase *1* by the reorientation of spin triangles within the spin plane.

Marchenko and Tikhonov [66] used the theory of exchange symmetry to show that the difference in the energies of phases *1* and *3* is determined by the same sixth-order relativistic invariant as the spectrum of the AFMR mode ω_{e3} [equations (17) and (18)], so that

$$\varepsilon_1 - \varepsilon_3 = 2F(H) = 2(b_1 + b_2H^2 + b_3H^4 + b_4H^6)\,.$$

At $H \cong H_{sf}$, all the terms in the sum are of the same order and the energy difference may change sign. Thus, the emergence of phase *3* agrees with the theory of the exchange symmetry of magnetic materials, but it remains to be seen whether such a phase appears in the phase diagram. However, we can calculate the energy of the spin chains with configurations of phases *1* and *3* with allowance for two exchanges and anisotropy, so that b_i can be expressed in terms of microscopic constants. A calculation done by Abarzhi et al. [13] has shown that the difference in the energies of these phases vanishes at $H = H_{sf}$ [equation (19)]. Their calculation, however, did not account for the difference in the mean spins of nonequivalent AF chains discovered in $CsMnI_3$. As shown in Ref. [44], allowance for this difference leads to the emergence of phase *3*.

As in Ref. [13], the magnetic energy is written in the form of a sum of energies of neighboring AF chains:

$$\varepsilon = -2j\sum_{\text{Axis}} S_iS_j - 2j'\sum_{\text{Plane}} S_iS_j\cos\beta_{ij} - D\sum_i S_i^2\cos^2\beta_i - \frac{H^2}{48j}\sum_i \sin^2\gamma_i\,, \tag{35}$$

where β_{ij} are the angles between the directions of the ith and jth spins, β_i are the angles between the ith spin and the C_6 axis, and γ_i are the angles between the ith spin and the external field. If we use equation (34) to calculate the values of the mean spins, then for $H \parallel C_6$ the above expression becomes

$$\varepsilon_1 = -3jS^2\left(1+\frac{\Delta^2}{2}\right) - 2j'S^2\left(1-\frac{\Delta}{2}\right) \times \left[2(1+\Delta)\cos\Theta - \left(1-\frac{\Delta}{2}\right)\cos 2\Theta\right] - \frac{H^2}{48j}\,2\sin^2\Theta - \frac{DS^2}{3}\left[(1+\Delta)^2 + 2\left(1-\frac{\Delta}{2}\right)^2\cos^2\Theta\right], \tag{36}$$

$$\varepsilon_3 = -3jS^2\left(1+\frac{\Delta^2}{2}\right) - 2j'S^2\left(1+\frac{\Delta}{2}\right) \times \left[2(1-\Delta)\sin\alpha + \left(1+\frac{\Delta}{2}\right)\cos 2\alpha\right] - \frac{H^2}{48j}\,(1+2\sin^2\alpha) - \frac{2DS^2}{3}\left(1+\frac{\Delta}{2}\right)^2\cos^2\alpha\,. \tag{37}$$

We derive the energy minimum condition with respect to the angles Θ and α between the spins and the C_6 axis (in the notation of Fig. 13) in the first order in Δ:

$$\cos\Theta = \left(1+\frac{3}{2}\,\Delta\right)\left[2-\frac{D}{3j'}\left(1-\frac{H^2}{H_{sf}^2}\right)\right]^{-1}, \tag{38}$$

$$\sin\alpha = \left(1-\frac{3}{2}\,\Delta\right)\left[2+\frac{D}{3j'}\left(1-\frac{H^2}{H_{sf}^2}\right)\right]^{-1}. \tag{39}$$

At $\Delta = 0$, equation (38) becomes the well-known expression (9) for the angles of the spin triangle; at $D/j' = 0$, these results coincide with the results of Marchenko and Tikhonov's calculations [62].

Substituting the expressions for the angles into (36) and (37), we find the difference in the energies of phases *1* and *3*, which after being normalized to DS^2 depends on three parameters: D/j', Δ, and H/H_{sf}. The analytical expressions are extremely cumbersome, so that here we give only the equation for b_1 [see equations (18) and (19)] and the result of numerical calculations of the function proper:

$$\varepsilon_1(0) - \varepsilon_3(0) = 2b_1 = -\frac{D^3S^2}{108j'^2}\left(1+54\frac{\Delta^2j'^2}{D}+12\frac{\Delta j'}{D}\right) \quad \text{at} \quad \frac{D}{j'} \leqslant 1\,. \tag{40}$$

Figure 18a shows the difference $\varepsilon_1 - \varepsilon_3$ at $D/j' = 0.6$ and $\Delta = 0.045$. Clearly, the difference changes sign at $H_C = 0.72H_{sf}$, i.e., the transition to phase *3* occurs sufficiently far from H_{sf}. Figure 18b displays the dependence $H_{C1}(\Delta)$ at $D/j' = 0.6$. As Δ decreases, H_C tends to H_{sf}. This means that phase *3* can exist only if the mean spins in the neighboring AF chains are different.

More precisely, the condition for the phase transition is the disappearance of the energy barrier between the phases.

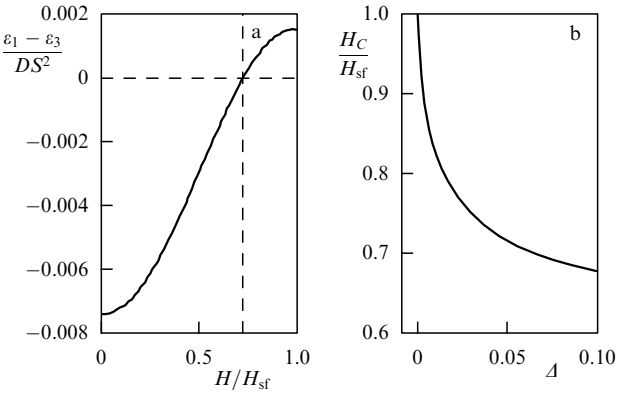

Figure 18. (a) Difference in energies of the first and third phases of $CsMnI_3$ as a function of the magnetic field, and (b) field of transition to phase *3* as a function of the difference of mean spins of nonequivalent AF chains [44].

But since in $CsMnI_3$ $\omega_{e3}^2 \propto F(H) = (\varepsilon_1 - \varepsilon_3)/2$, the fact that the energies are equal implies that there is no energy barrier.

To compare these results with the experimental data, one needs to know D/j'. Until now, the various experiments yielded different values of this ratio. Harrison et al. [46] determined D and j' directly from spin-wave spectra: $D/j' = 0.5$. Another approach amounts to measuring the ratio of the gaps of the AFMR modes: $\omega_{e1}/\omega_{e3} \propto \sqrt{b_1}$. Using equation (40) to find b_1, we obtain $D/j' = 0.6$. This magnitude coincides with the inelastic neutron scattering data of Harrison et al. [46] to within the accuracy of the data and is, we believe, the most meaningful.

The same parameter determines the angles between the spins of neighboring AF chains, which, according to neutron diffraction data, is $\Theta(0) = 51^\circ \pm 1^\circ$ [45, 46]. However, in the calculations of the neutron scattering intensities, the anisotropy of the spins of Mn in the AF chains was ignored. It can easily be shown that allowance for this anisotropy increases the angle by

$$\frac{\delta \sin\Theta}{\sin\Theta} \approx \frac{\Delta S}{S},$$

i.e., the correct value is equal to $\Theta(0) = 52^\circ - 54^\circ$, which is close to the ^{55}Mn NMR data.

The field behavior of the angle Θ between the spins in the low-field phase at $D/j' \approx 0.6$ and $\Delta = 0.045$ is depicted in Fig. 16. Clearly, the result is in good agreement with the experimental data. For the same values of the parameters, we obtain $H_C = 37.8$ kOe, which is in good agreement with the experimental value $H_C = 39$ kOe.

Consequently, the allowance for the anisotropy of spin reduction in Mn makes it possible not only to explain the emergence of the intermediate magnetic phase *3*, but also removes the well-known contradictions [13] in calculations that are based on the model Hamiltonian (6).

Within this model, one can calculate the dependence of H_{C1} on the angle φ between the external field and the C_6 axis. To this end, in equation (35) one takes into account the dependence of the angles β_i and γ_i on φ and ψ (the angle between the normal to the spin plane and the C_6 axis). This changes the last two terms on the right-hand sides of equations (36) and (37), so that they become

$$\varepsilon_1 = \ldots - \frac{H^2}{48j}\left\{\cos^2(\psi-\varphi) + 2\left[1 - \sin^2(\psi-\varphi)\cos^2\Theta\right]\right\} - \frac{DS^2}{3}\left[(1+\Delta)^2\sin^2\psi + 2\left(1-\frac{\Delta}{2}\right)^2\cos^2\Theta\sin^2\psi\right], \quad (41)$$

$$\varepsilon_3 = \ldots - \frac{H^2}{48j}\left[3 - 2\sin^2(\psi-\varphi)\cos^2\alpha\right] - \frac{2DS^2}{3}\left(1+\frac{\Delta}{2}\right)^2\cos^2\alpha\,\sin^2\psi\,. \quad (42)$$

Then ε_1 and ε_3 are minimized with respect to this angle and the results are compared. Figure 19 shows the results of the calculations and the results of measurements. The experimental dependence $H_C(\varphi)$ is somewhat steeper, and at $\varphi = 20^\circ$ there is no transition to phase *3*, but qualitatively the results coincide. Note that the resulting field dependence $\psi(H)$ for both phases is close to that calculated by Abarzhi et al. [13] [equation (10)] and agrees well with the data of the NMR experiment (see Fig. 14).

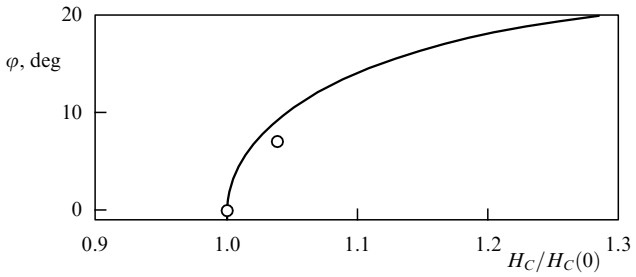

Figure 19. Field of transition to phase *3* as a function of the angle between the field and the C_6 axis [44]. The circles represent the results of the experiment described in Ref. [36].

Thus, allowance for the anisotropy of mean-spin reduction makes it possible to describe the set of the low-temperature magnetic properties of $CsMnI_3$. We can assume that this approach can be applied to other easy-axis triangular antiferromagnets

The intermediate phase *3*, discovered in $CsMnI_3$ in fields applied at small angles to the C_6 axis, exists due to the anisotropy of the mean spins of nonequivalent AF chains. This anisotropy is a consequence of the anisotropy of the quantum fluctuations in quasi-one-dimensional six-sublattice antiferromagnets. Until now, only two cases of magnetically ordered structures whose existence is due to quantum fluctuations were known: the high-field phase in $CsCuCl_3$ for $H \,||\, C_6$ [67, 68] and the 'stripe' phase in CaV_3O_7 [69, 70]. In contrast to these substances, $CsMnI_3$ is a very simple compound with a perfect hexagonal structure. The emergence of a new magnetic phase due to the effect of the anisotropy of quantum fluctuations has been observed for the first time. Possibly, there exists an analogy between our results and Chubukov's model for two-dimensional antiferromagnetic structures [71], where the intermediate phase acquires a finite (in the magnetic field) region of existence owing to the effect of quantum fluctuations.

7. Conclusions

Quantum fluctuations have a drastic effect on the magnetic properties of quasi-one-dimensional triangular antiferromagnets, including the initiation of new phase transitions without disrupting the magnetic order. The behavior of magnetization in a magnetic field agrees semiquantitatively, and that of the mean spins of the sublattices agrees qualitatively, with the spin-wave theory of quantum fluctuations. A detailed comparison requires microscopic calculations of the suppression of spin reduction by the field in situations close to the experimental one. Our hope is that theoreticians will be interested in the fairly detailed results presented in this review that concern the field dependence of the mean spins and their anisotropy in magnetically nonequivalent AF chains.

The field for further experiments is broad. For instance, it is important to study the magnetic phase diagram of $CsMnI_3$ at higher temperatures. If phase *3* exists up to the multicritical point, the entire concept of the latter may change. It would also be interesting to search for this phase in other easy-axis triangular antiferromagnets, in particular in $CsNiBr_3$, where D/j' is fairly large. Continuing the experiments on the field dependence of mean spins in stronger magnetic fields would also be useful. In particular, it would be interesting to see whether the anisotropy of spin reduction for $H \perp C_6$ is

retained up to exchange fields. Such investigations are important for both easy-plane and easy-axis triangular antiferromagnets.

I dedicate this review to the memory of A S Borovik-Romanov, who initiated and guided many investigations covered in the review. Paper [35] was the last written by Borovik-Romanov. I am deeply grateful to A F Andreev for the opportunity to carry out the present research at the Kapitza Institute of Physic Problems of the Russian Academy of Sciences, to A M Tikhonov with whom I carried out the ^{55}Mn NMR experiments, to S V Petrov for preparing the samples, and to V A Panfilov for the help in preparing the manuscript. The work was supported in part by the Russian Foundation for Basic Research, project 97-02-16795.

References

1. Borovik-Romanov A S, in *Itogi Nauki* (Results in Science), Ser.: Fiz.-Mat. Nauki, No. 4, Dorfman Ya G (Ed.) (Moscow: Izd. Akad. Nauk SSSR, 1962) p. 35
2. Anderson P W *Phys. Rev.* **86** 694 (1952)
3. Welz D *J Phys.: Condens. Matter* **5** 3643 (1993)
4. Ishikawa T, Ogychi T *Prog. Theor. Phys.* **54** 1282 (1975)
5. Aleksandrov K S et al. *Fazovye Perekhody v Kristallakh Galoidnykh Soedineniĭ ABX_3* (Phase Transitions in Crystals of ABX_3 Halide Compounds) (Novosibirsk: Nauka, 1981)
6. Collins M F, Petrenko O A *Can. J. Phys.* **75** 605 (1997)
7. Chubukov A V *J. Phys. C: Solid State Phys.* **21** 441 (1988)
8. Abarzhi S et al. *J. Phys.: Condens. Matter* **4** 3307 (1992)
9. Eibishutz M et al. *AIP Conf. Proc.* **17** 864 (1972)
10. Gaulin B D et al. *Phys. Rev. Lett.* **62** 1380 (1989)
11. Xu X et al. *J. Phys.: Condens. Matter* **8** L371 (1996)
12. Kawamura H *J. Phys.: Condens. Matter* **10** 4707 (1998)
13. Abarzhi S I et al. *Zh. Eksp. Teor. Fiz.* **104** 3232 (1993) [*JETP* **77** 521 (1993)]
14. Katori H A, Goto T, Ajiro Y *J. Phys. Soc. Jpn.* **62** 743 (1993)
15. Tanaka H et al. *J. Phys. Soc. Jpn.* **58** 2930 (1989)
16. Zaliznyak I, Prozorova L, Petrov S *Zh. Eksp. Teor. Fiz.* **97** 359 (1990) [*Sov. Phys. JETP* **70** 203 (1990)]
17. Kimura S, Ohta H, Motokawa M *J. Phys. Soc. Jpn.* **66** 4027 (1997)
18. Tanaka H et al. *J. Phys. Soc. Jpn.* **57** 3979 (1988)
19. Andreev A F, Marchenko V I *Usp. Fiz. Nauk* **130** 39 (1980) [*Sov. Phys. Usp.* **23** 21 (1980)]
20. Cambe T, Tanaka H, Nagata K *J. Phys. Soc. Jpn.* **62** 3388 (1993)
21. Kambe T et al. *J. Phys. Soc. Jpn.* **65** 1799 (1996)
22. Zaliznyak I *Solid State Commun.* **84** 573 (1992)
23. Abanov A G, Petrenko O A *Phys. Rev. B* **50** 6271 (1994)
24. Ohyama T, Shiba H *J. Phys. Soc. Jpn.* **63** 3454 (1994)
25. Zhitomirsky M, Zaliznyak I *Phys. Rev. B* **53** 3428 (1996)
26. Watabe Y, Suzuki T, Natsume Y *Phys. Rev. B* **52** 3400 (1995)
27. De-Gennes P G et al. *Phys. Rev.* **129** 1105 (1963)
28. Turov E A, Kuleev V G *Zh. Eksp. Teor. Fiz.* **49** 248 (1965) [*Sov. Phys. JETP* **22** 176 (1966)]
29. Turov E A, Petrov M P *YaMR v Ferro- i Antiferromagnetikakh* (Nuclear Magnetic Resonance in Ferro- and Antiferromagnets) (Moscow: Nauka, 1969) Chap. 2 [Translated into English (Jerusalim: Israel Program for Scientific Translations, 1972)]
30. Welsh L B *Phys. Rev.* **156** 370 (1967)
31. Zaliznyak I, Zorin N, Petrov S *Pis'ma Zh. Eksp. Teor. Fiz.* **64** 473 (1996) [*JETP Lett.* **64** 473 (1996)]
32. Tikhonov A M, Author's abstract of of Ph. D. thesis in Physics and Mathematics) (Moscow: Institut Fiz. Problem im. P L Kapitsy RAN, 1998)
33. Dumesh B S, Petrov S V, Tikhonov A M *Pis'ma Zh. Eksp. Teor. Fiz.* **67** 661 (1998) [*JETP Lett.* **67** 692 (1998)]
34. Gurevich G M et al. *Zh. Eksp. Teor. Fiz.* **84** 823 (1983) [*Sov. Phys. JETP* **57** 477 (1983)]
35. Borovik-Romanov A S et al. *Zh. Eksp. Teor. Fiz.* **113** 352 (1998) [*JETP* **86** 197 (1998)]
36. Dumesh B S, Petrov S V, Tikhonov A M *Pis'ma Zh. Eksp. Teor. Fiz.* **67** 988 (1998) [*JETP Lett.* **67** 1046 (1998)]
37. Dumesh B S, Kirkin M I, Petrov S V, Tikhonov A M *Zh. Eksp. Teor. Fiz.* **115** 2228 (1999) [*JETP* **88** 1221 (1999)]
38. Prozorova L A et al. *Zh. Eksp. Teor. Fiz.* **112** 1893 (1997) [*JETP* **85** 1035 (1997)]
39. Dumesh B S *Prib. Tekh. Eksp.* (1) 135 (1986)
40. Borovik-Romanov A S et al. *Pis'ma Zh. Eksp. Teor. Fiz.* **66** 759 (1997) [*JETP Lett.* **66** 759 (1997)]
41. McPherson G, Koch R C, Stucky G D *J. Chem. Phys.* **60** 1424 (1974)
42. Kubo T, Miyakita J, Maegawa S *J. Magn. Magn. Mater.* **177 – 181** 829 (1998)
43. Govorkov S, Tulin V *Pis'ma Zh. Eksp. Teor. Fiz.* **37** 383 (1983) [*JETP Lett.* **37** 454 (1983)]
44. Dumesh B, Panfilov V, Fourzikov D *Phys. Rev. B* (to be published)
45. Zandbergen H W *J. Solid State Chem.* **35** 367 (1980)
46. Harrison A et al. *Phys. Rev. B* **43** 679 (1991)
47. Dumesh B et al. *Physica B* **284** 1623 (2000)
48. Tzihtnyuk Yu, in "*EPDIS-6*" (Budapest, 1998) p. 83
49. Glinka C J et al. *AIP Conf. Proc.* **10** 684 (1973)
50. Heller L et al. *Phys. Rev. B* **49** 1104 (1994)
51. Bazhan A N et al. *Zh. Eksp. Teor. Fiz.* **103** 691 (1993) [*JETP* **76** 342 (1993)]
52. Vitebskiĭ I M et al. *Zh. Eksp. Teor. Fiz.* **103** 326 (1993) [*JETP* **76** 178 (1993)]
53. Kirklin K H, McPherson G L *J. Phys. C* **16** 6539 (1983)
54. Geshwind S, in *Hyperfine Interactions* (Eds. A J Freeman, R B Frankel) (New York: Academic Press, 1967)
55. Watson R, Freeman A J, in *Hyperfine Interactions* (Eds A J Freeman, R B Frankel) (New York: Academic Press, 1967)
56. Ogawa S *J. Phys. Soc. Jpn.* **15** 1475 (1960)
57. Abragam A, Pryce M H L *Proc. R. Soc. London Ser. A* **205** 135 (1951)
58. Taylor D R, Owen J *Phys. Rev. Lett.* **17** 159 (1966)
59. Huang N L, Orbach R, Simanek E *Phys. Rev. Lett.* **17** 134 (1966)
60. Raine J A, Collins J F, White G K *J. Appl. Phys.* **55** 2404 (1984)
61. Natsume Y, Private communication
62. Marchenko V I, Tikhonov A M *Pis'ma Zh. Eksp. Teor. Fiz.* **69** 41 (1999) [*JETP Lett.* **69** 44 (1999)]
63. Plumer M J,Caille A, Hood K *Phys. Rev. B* **39** 4489 (1989)
64. Plumer M J, Caille A *J. Appl. Phys.* **70** 5961 (1991)
65. Zhitomirskiĭ M E *Zh. Eksp. Teor. Fiz.* **108** 343 (1995) [*JETP* **81** 185 (1995)]
66. Marchenko V I, Tikhonov A M *Pis'ma Zh. Eksp. Teor. Fiz.* **68** 844 (1998) [*JETP Lett.* **68** 887 (1998)]
67. Stnesser N et al. *Physica B* **213 – 214** 164 (1995)
68. Nikuni T, Shiba H *J. Phys. Soc. Jpn.* **62** 3268 (1993)
69. Harashina H, Kodama K *J. Phys. Soc. Jpn.* **65** 1570 (1996)
70. Kontani H, Zhitomirsky M, Ueda K *J. Phys. Soc. Jpn.* **65** 1566 (1996)
71. Chubukov A V et al. *J. Phys.: Condens. Matter.* **3** 69 (1991)